Optical Display of the Airy Function and Transient Wave Propagation in a Dispersive Medium

by

Jeong-Han Kim

Thesis submitted to the Faculty of the

Virginia Polytechnic Institute and State University

in partial fulfillment of the requirements for the degree of

Master of Science

in

Electrical Engineering

APPROVED:

Dr. T.-C. Poon, Chairman

Dr. I. M. Besieris

Dr. G. Indebetouw

1996
Blacksburg, Virginia

Key words : Diffraction, Dispersion relation, FFT, Fourier transformation, Intensity variation

LD
S655
V855
1996
K559
c.2

Optical Display of the Airy Function and Transient Wave Propagation in a Dispersive Medium

by

Jeong-Han Kim

Committee Chairman : Dr. Ting-Chung Poon

Electrical Engineering

(ABSTRACT)

The display of an Airy function via an optical image processing technique is demonstrated. using a two-dimensional object with a cubic amplitude transmittance, one can observe a Fourier transformed image of which intensity variation is identical to that of the Airy function. A lens system is used to achieve the Fourier transformation of the object which is a two-dimensional binary filter. A set of computer simulations are performed prior to the optical experiments.

Using the same method of optical display, the transient wave propagation in a dispersive medium is optically displayed based on the analogous relationship found between two equations: One is the Fourier form of a transient wave field propagating in a dispersive medium and the other is an equation of the diffraction pattern of an object constructed with two juxtaposed two-dimensional filters. A theoretical analysis is provided along with computer simulations. The use of a Spatial Light Modulator is proposed as the source of the input object in the optical experiment.

ACKNOWLEDGMENTS

I would like to extend my thanks and appreciation to many people whose help I received throughout this endeavor. First, I wish to express my gratitude to my chair and advisor Dr. T. -C. Poon for his advice, guidance and effort devoted to this research. I am also indebted to Dr. I. M. Besieris and Dr. G. Indebetouw for their encouragement, enthusiasm and generous assistance throughout my program.

In addition, I would like to acknowledge my fellow students work in the Optical Image Processing lab for their suggestions and help on my thesis. Special thanks to Mr. Xia who helped me in a number of late night experiments and Brad for his encouragement.

Special thanks are directed to my family in Seoul, Korea for their endless support. Without their support this master's thesis would not be possible.

Finally, my deepest appreciation is devoted to my wife Jeonglim to whom this thesis is dedicated.

TABLE OF CONTENTS

ABSTRACT ii

ACKNOWLEDGMENTS iii

LIST OF FIGURES vii

LIST OF TABLES ix

Chapter 1 INTRODUCTION 1

Chapter 2 THEORETICAL BACKGROUND 3

2.1 Fresnel Integral and Fourier Transform 3

2.2 Fourier Transform of an Object in an Optical setup 6

2.3 Optical Display of the Airy Function 7

Chapter 3 SIMULATIONS 11

3.1 Construction of a 2D Object Matrix 12

3.2 Two-Dimensional Fourier Transformation of an Object Matrix 12

3.3 Tracing of the Amplitude Variation on the Image Plane 13

3.4 Effect of Thickness of the Transparent Region 17

Chapter 4 **OPTICAL EXPERIMENT** 22

4.1 System A and Observation..... 22

4.1.1 Object Image Filter..... 23

4.1.2 2D Fourier Transform..... 25

4.2 System B and Intensity Measurement..... 27

4.3 Result from Optical Setup..... 31

4.3.1 Magnification of L2..... 31

4.3.2 Generation of the Airy Function with Experimental Parameters..... 32

4.4 Discussion of the Output..... 34

4.4.1 Error due to the thickness of the transparent region..... 34

4.4.2 Noise from the characteristic properties of the light wave.. 34

Chapter 5 **OPTICAL DISPLAY OF THE PROPAGATION OF A TRANSIENT WAVE IN A DISPERSIVE MEDIUM**..... 36

5.1 Transient Wave Propagation in a Dispersive Medium..... 36

5.2 Simulation of Transient Wave Propagation 41

Chapter 6 **OPTICAL PROCESSING USING AN EBSLM**..... 47

Chapter 7 **CONCLUSION**..... 53

6.1 Summary 53

6.2 Further Studies 54

6.3 System Improvement 54

REFERENCES 55

APPENDIX A 57

VITA 61

LIST OF FIGURES

Figure		Page
2.1	Diffraction geometry	5
2.2	Fourier Transformation of a 2D object using a lens system	5
2.3	Reading amplitude variation of the Fraunhofer diffraction pattern	10
3.1	2D object matrix with the size of 512*512	14
3.2	2D Fast Fourier Transformed image matrix	15
3.3	Intensity variation of a row vector from figure 3-2	16
3.4	Sampled intensity variation on the 10th row vector from the center (width applied : 4 pixels)	19
3.5	Sampled intensity variation on the 10th row vector from the center (width applied : 8 pixels)	20
3.6	Sampled intensity variation on the 10th row vector from the center (width applied : 15 pixels)	21
4.1	Optical set-up for the observation of diffraction pattern	23
4.2	2D binary object of the system A (8 mm width for both sides)	24
4.3	Optical set-up for intensity measurement	26
4.4	Optically produced Fraunhofer diffraction pattern of the 2D binary object	29
4.5	Intensity variation based on the data of table 4-1	30

4.6 (a) Airy function theoretically constructed by experimental parameters.. 33

(b) Qualitative comparison of Figure 4-5 and 4-6 a..... 33

5.1 Two juxtaposed masks containing the information about the Dispersive relation and the spatial spectrum of the transient wave propagating in a Dispersive medium..... 40

5.2 Result of 2D FFT of T(x,y) with 1D Gaussian characteristics..... 43

5.3 (a) Intensity variation from the row vector located at the center of the image..... 44

(b) Intensity variation of the 14th vector from the center of the image..... 44

(c) Intensity variation of the 28th vector from the center of the image..... 45

(d) Normalized intensity variation pattern of different time constant..... 46

6.1 Set-up using an EBSLM..... 49

6.2 EBSLM input amplitude transmittance..... 50

6.3 Diffraction pattern of the 2D object from an EBSLM..... 51

6.4 Intensity variation of Figure 5-6 created by a computer reading of CCD image..... 52

LIST OF TABLES

Tables **Page**

4.1 Intensity variation of diffraction pattern..... 28

Chapter 1

INTRODUCTION

One of the most remarkable and useful properties of optical image processing is the formation of a two-dimensional Fourier transformation with a simple coherent optical imaging system. Based on this property, a number of applications have been made recently in optically displaying mathematical functions. [1][2][3] It is the intent of this thesis to introduce the technique of the optical display and to show that the technique can be applied for an optical scheme for the optical display of the one-dimensional space time evolution of a wave packet in a dispersive medium with an example of cubic dispersion relation. The optical display method is introduced with an example of displaying an Airy function which is sampled from the diffraction pattern of a two-dimensional object containing the cubic relation.

Our discussion is focused on the data from simulations and the experimental parameters, and it includes other related areas, such as the technique of two-dimensional optical Fourier transformation, electro-optics, and numerical data analysis. The contents of this thesis can be divided into three main parts: First, qualitative data related to experimental parameters are gathered from simulations. Second, an optical set-up for parallel display of Airy functions is presented. Third, an optical display of transient wave propagation in a dispersive medium is exhibited.

It is appropriate to discuss some of the underlying theoretical concepts before presenting experimental results. In Chapter 2, theoretical background regarding the optical display of the Airy function is presented. Starting with the Fresnel diffraction equation, basic explanations for producing a Fraunhofer diffraction pattern are reviewed. The concept of trading a dimension for displaying the Airy function is also discussed. [3][4]

As mentioned earlier, data simulations using a personal computer are performed prior to the actual experiments. Using these data simulations, the effect of a parameter change on the diffraction pattern is analyzed qualitatively. In Chapter 3, the procedure of simulations is presented and the effect of a parameter change is discussed. Programmed codes for the simulations are provided in the appendix.

Procedures and results of conducted optical experiments are presented in Chapter 4. Based on the theoretical background of Chapter 2, the Fraunhofer diffraction pattern of a two-dimensional object is observed and detected using a lens system. The experiments are conducted in two parts with two different set-ups. We call them System A and System B to avoid confusion. System A is a set-up for the observation of the resulting image pattern and System B is used for the measurement of the intensity of the image. Expected data from the simulations in Chapter 3 are compared with experimental results.

As an additional application of the optical display method, transient wave propagation in a dispersive medium is simulated in Chapter 5. The theoretical analysis includes an analogy between the variables of the Fourier-transformed equation for a propagating wave in a dispersive medium and the parameters of the Fraunhofer diffraction pattern of two juxtaposed binary objects. A set of computer simulations is conducted to support the theoretical analysis. To avoid the limitation of the photo-film based binary objects and to benefit from the ability of input object manipulation, a Spatial Light Modulator is adopted in the optical system as the source of the input object. The results of the optical experiment are discussed.

Concluding remarks are presented in Chapter 7. Based on procedures and data discussed in previous chapters, a summary of our discussion is provided and methods for system improvement are presented.

Chapter 2

THEORETICAL BACKGROUND

2.1 Fresnel Integral and Fourier Transformation

From Huygen-Fresnel's principle and as shown in Figure 2-1, the field amplitude at point (x, y) is expressed as

$$U(x,y) = \frac{exp(jkz)}{j\lambda z}\int\int_{-\infty}^{\infty} U(x_o, y_o) exp\{j\frac{k}{2z}[(x-x_o)^2 + (y-y_o)^2]\}dx_o dy_o, \qquad (2\text{-}1\text{-}1)$$

where $k = \frac{2\pi}{\lambda}$ is the optical wave number with λ the optical wavelength, and $U(x_o, y_o)$ is the aperture function on the x_o-y_o plane. This equation involves a convolution of $U(x_o, y_o)$ and a free space impulse response function [6, 7]

$$h(x,y,z) = \frac{-j}{\lambda z} exp(jkz) exp\{j\frac{k}{2z}(x^2+y^2)\}. \qquad (2\text{-}1\text{-}2)$$

Note that Eq. (2-1-1) is derived under the usual paraxial approximation. [7] After the expansion of quadrature terms in Eq. (2-1-1), we have

$$U(x,y) = \frac{exp(jkz)}{j\lambda z} exp[j\frac{k}{2z}(x^2+y^2)]\int\int_{-\infty}^{\infty} U(x_o, y_o) exp[j\frac{k}{2z}(x_o^2+y_o^2)] exp[-j\frac{k}{z}(xx_o + yy_o)]dx_o dy_o. \qquad (2\text{-}1\text{-}3)$$

The diffraction pattern given in Eq. (2-1-3) can be simplified when the distance z is such that [7]

$$z \gg \frac{k(x_o^2+y_o^2)_{\max}}{2}; \qquad (2\text{-}1\text{-}4)$$

the latter is the Fraunhofer condition. Under this assumption, Eq. (2-1-3) becomes

$$U(x,y) \simeq \frac{exp(jkz)}{j\lambda z} exp[j\frac{k}{2z}(x^2+y^2)] \int_{-\infty}^{\infty}\int_{-\infty}^{\infty} U(x_o, y_o) exp[-j\frac{k}{z}(xx_o + yy_o)] dx_o dy_o. \qquad (2\text{-}1\text{-}5)$$

Disregarding the phase factor outside the integral, the equation above shows the Fourier transform of the aperture function $U(x_o, y_o)$; specifically,

$$FT\{U(x_o, y_o)\} = \int_{-\infty}^{\infty}\int_{-\infty}^{\infty} U(x_o, y_o) exp[-j2\pi(\alpha x_o + \beta y_o)] dx_o dy_o, \qquad (2\text{-}1\text{-}6)$$

with spatial frequency variables $\alpha = \frac{1}{\lambda z}x, \beta = \frac{1}{\lambda z}y$.

In order to have a Fraunhofer diffraction pattern of an aperture with 1 cm of width on each side, the observation distance needs to be large; for λ=632.8 nm it follows from Eq. (2-1-4) that

$$\frac{k(x_o^2+y_o^2)_{\max}}{2} = \frac{2\pi}{632.8 \text{ nm}} \frac{(\frac{1.0}{2}*0.01)^2+(\frac{1.0}{2}*0.01)^2}{2} \simeq 248.2\text{m}, \qquad (2\text{-}1\text{-}7)$$

and this suggests that z $\gg$ 248.2 m is needed in order to observe optical Fourier transformation. From a practical point of view, we need to apply a lens for reducing the observation distance.

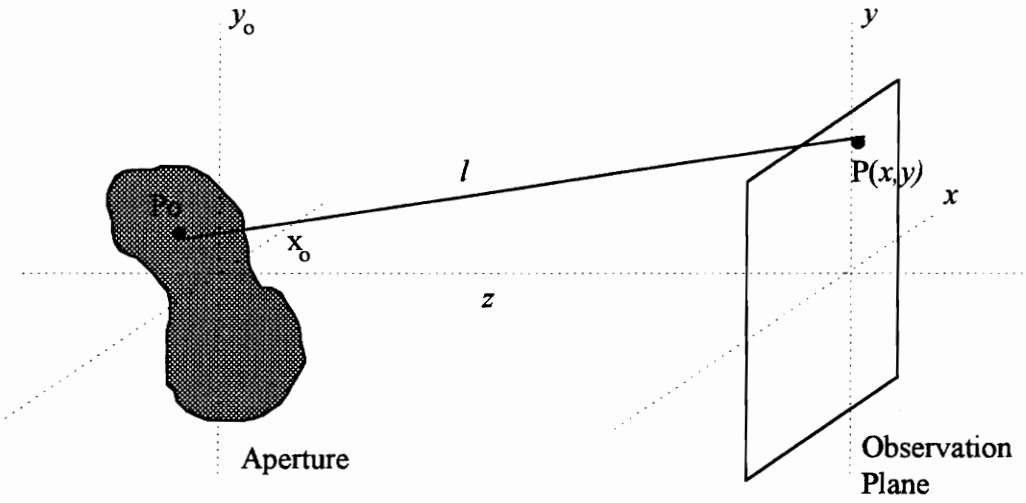

Figure 2-1 Diffraction Geometry

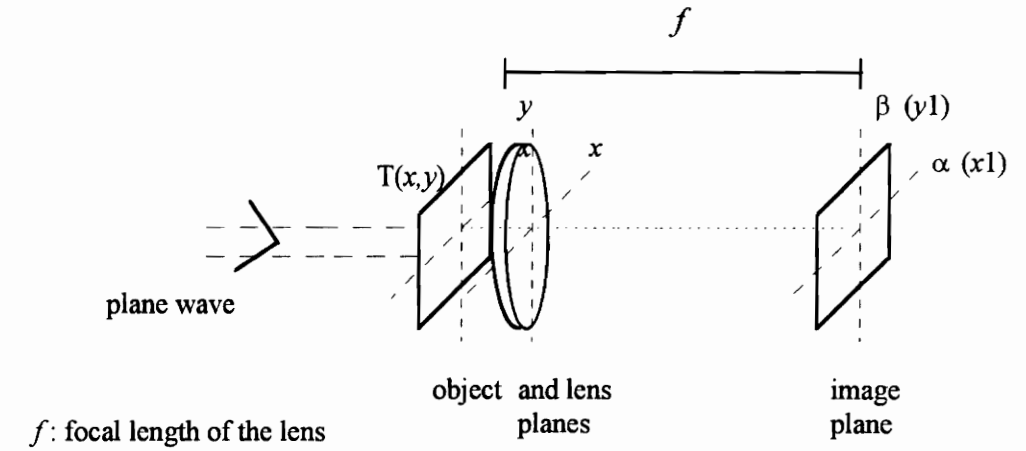

Figure 2-2 Fourier transform of an 2D object using a lens system

2.2 Fourier Transform of an Object in an Optical Set-up

Optical Fourier transformation can be achieved without having a large distance between the aperture and the observation plane. Phase transformation of a (thin) double-convex lens is known to be described as the function [6, 7]

$$\Phi(x,y) = exp(-j\tfrac{k}{2f}(x^2+y^2)), \qquad (2\text{-}2\text{-}1)$$

where f is the focal length of the lens.

Let $T(x,y)$ be the amplitude transmittance of a 2D object placed immediately in front of the converging lens, as shown in Figure 2-2. With a unit plane wave illuminating the object, the amplitude distribution behind the lens becomes

$$U_b(x,y) = T(x,y)exp(-j\tfrac{k}{2f}(x^2+y^2)). \qquad (2\text{-}2\text{-}2)$$

Applying the Fresnel diffraction equation [cf. Eq. (2-1-3)], the distribution on the back focal plane becomes

$$U_f(x_1,y_1) = \frac{exp(jkf)}{j\lambda f}exp[j\tfrac{k}{2f}({x_1}^2+{y_1}^2)]\int\int_{-\infty}^{\infty}U_b(x,y)exp[j\tfrac{k}{2f}(x^2+y^2)]exp[-j\tfrac{k}{f}(xx_1+yy_1)]dxdy. \qquad (2\text{-}2\text{-}3)$$

In terms of $\alpha = \frac{1}{\lambda f}x_1$ and $\beta = \frac{1}{\lambda f}y_1$, Eq. (2-2-3) assumes the form

$$U_f(\alpha,\beta) = \frac{exp(jkf)}{j\lambda f}exp[j\lambda f\pi(\alpha^2+\beta^2)]\int\int_{-\infty}^{\infty}U_b(x,y)exp[j\tfrac{k}{2f}(x^2+y^2)]exp[-j2\pi(x\alpha+y\beta)]dxdy.$$

(2-2-4)

Substituting Eq. (2-2-2) into $U_f(\alpha,\beta)$, $exp[j\frac{k}{2f}(x^2+y^2)]$ and the exponential term in $\Phi(x,y)$ cancels each other. We have, then,

$$U_f(\alpha,\beta) = \frac{exp(jkf)}{j\lambda f} exp[j\lambda f\pi(\alpha^2+\beta^2)] \int\int_{-\infty}^{\infty} T(x,y) exp[-j2\pi(x\alpha+y\beta)]dxdy$$
$$= \frac{exp(jkf)}{j\lambda f} exp[j\lambda f\pi(\alpha^2+\beta^2)] FT\{T(x,y)\}, \qquad (2\text{-}2\text{-}5)$$

It is seen that Eq. (2-2-5) has the form of a Fourier transformation of $T(x,y)$, with a phase factor preceding the integral. Since only the intensity variation is to be measured, the exponential term in the phase distribution plays no role. The intensity of $U_f(\alpha,\beta)$ is given by

$$I(\alpha,\beta) = |U_f(\alpha,\beta)|^2$$

$$= \frac{1}{(\lambda f)^2} \left| \int\int_{-\infty}^{\infty} T(x,y) exp[-j2\pi(x\alpha+y\beta)]dxdy \right|^2_{\alpha=\frac{x_1}{\lambda f},\beta=\frac{y_1}{\lambda f}}$$

$$= \frac{1}{(\lambda f)^2} |FT[T(x,y)]|^2. \qquad (2\text{-}2\text{-}6)$$

2.3 Optical Display of the Airy Function

Let us examine the optical Fourier transformation system shown in Figure 2-3. A plane wave coming from a collimator illuminates a 2-D object, and the object is a binary screen which is transparent only along the line of an intended function $y=F(x)$. The Fourier transformed image of the 2D object appears on the image plane, and the intensity

is measured by a photo-detector. The amplitude transmittance of the object can be represented as [1]

$$T(x,y) = \delta(y - F(x)), \qquad (2\text{-}3\text{-}1)$$

where $\delta(\ )$ denotes a Dirac delta function. Based on the Fraunhofer diffraction theory, the lens system creates the Fourier transformed image of $T(x,y)$ on the output plane (α,β). From Eq. (2-1-6), the output is given by

$$FT\{T(x,y)\} = \int_{-\infty}^{\infty}\int_{-\infty}^{\infty} exp(-j2\pi(\alpha x + \beta y))\delta(y - F(x))dxdy$$

$$= \int_{-\infty}^{\infty} exp(-j2\pi(\alpha x + \beta F(x))dx. \qquad (2\text{-}3\text{-}2)$$

Using a binary mask for *T(x, y)*, it is possible to produce a Fraunhofer diffraction pattern which has an amplitude variation related to a desired mathematical function, e.g., the Airy function, [1][2][3]. From the integral definition of the Airy function, [8] we have

$$2\pi(3\epsilon)^{-\frac{1}{3}} Ai[(\pm(3\epsilon)^{-\frac{1}{3}}\tau] = \int_{-\infty}^{\infty} exp(-j(\epsilon t^3 \pm \tau t))dt. \qquad (2\text{-}3\text{-}3)$$

By comparing equation (2-3-2) with (2-3-3), we identify

$$F(x) = cx^3, \qquad (2\text{-}3\text{-}4)$$

where c is an arbitrary constant.

Substituting equation (2-3-4) into (2-3-2), the diffraction pattern is given by

$$FT\{T(x,y)\} = \int_{-\infty}^{\infty}\int_{-\infty}^{\infty} exp(-j2\pi(\alpha x+\beta y))\delta(y-cx^3)dxdy$$

$$= \int_{-\infty}^{\infty} exp(-j2\pi(\alpha x+\beta cx^3))dx$$

$$= 2\pi(6\pi c\beta)^{-\frac{1}{3}} Ai[(6\pi c\beta)^{-\frac{1}{3}}2\pi\alpha]. \qquad (2\text{-}3\text{-}5)$$

The intensity of the image plane is read as

$$I(\alpha,\omega) = \{2\pi(6\pi c\beta)^{-\frac{1}{3}}\}^2[\,Ai\{(6\pi c\beta)^{-\frac{1}{3}}2\pi\alpha\}]^2\,|_{\beta=\omega}, \qquad (2\text{-}3\text{-}6)$$

for a fixed value of β.

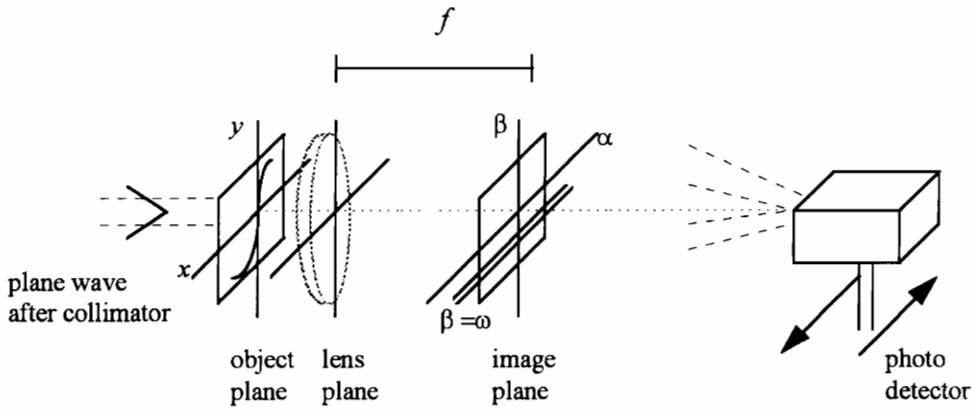

focal length of the lens : 680 mm
wave length of plane wave : 632.8 nm

Figure 2-3 Reading amplitude variation of the Fraunhofer diffraction pattern

Chapter 3

SIMULATIONS

It is possible to predict the outcome of an optical experiment and to adjust parameters accordingly with the help of simulations using a high speed digital computer. Having the advantage of parameter control without the difficulty of physical equipment change, an overview of the experimental outcome is allowed from various aspects. In our case, the location of the observation point and the shape of the input amplitude transmittance function are prominent parameters to be controlled.

From Chapter 2, the amplitude transmittance of the input object has been defined as

$$T(x, y) = \delta(y - F(x)), \qquad (3\text{-}1\text{-}1)$$

with $F(x) = cx^3$ as a specific choice leading to the Airy function.

Notice that the input object of the experiment is a two-dimensional mask, only transparent along the $y = F(x)$ line. The input object with the given amplitude transmittance is referred to as the input mask, which is a photo-film based filter in the experimental set-ups. According to the Eqs. (2-3-6) and (2-3-7), the output intensity of the optical Fourier transformer is measured by sampling a row of data from the parallel display of a 2D Airy function pattern. Based on the aspects described above, the basic requirements for the simulation procedure can be summarized as follows:

* Creating a digitized input mask according to the theoretical analysis;

* Performing a 2D Fourier transform;
* Sampling the intensity in the image plane.

3.1 Construction of a 2D Digitized Input Mask

A 2D digitized input mask is constructed by an array of small pixels which form a 2D matrix. The matrix is called the object matrix. Each element of the object matrix contains information regarding the intensity and the location of each pixel. The intensity level of a single pixel can be chosen from 64 levels of gray scale (0~63). [10][11]

The 2D object matrix contains the function $T(x, y)$ of Eq. (3-1-1). The contrast of the matrix is maximized by having the highest intensity level along the function $F(x)$ and the lowest level (zero intensity) on the rest of the matrix. The size of the matrix determines the resolution, which affects smoothness and accuracy of the simulated data. Even if it is more desirable to have higher resolution, we should not overlook the fact that the simulation process involving matrices with high resolution requires a substantial amount of extra computation and time, as well as memory capacity of the computer. The size of the matrix is set at 512*512 for our simulations. Figure 3-1 shows the image of the object matrix created by a computer with $c = \frac{1}{3}$.

3.2 Two-Dimensional Fourier Transformation of the Object Matrix

A two-dimensional Fourier transform is performed via a two dimensional Fast Fourier Transformation (FFT2). FFT2 is the command for the 2D Fourier transform and it returns Fourier transformed values of each element of the 2D matrix. Figure 3-2 shows the result of the two-dimensional Fast Fourier transformation of a 2D object matrix. [11][12] According to Eq. (2-3-5), the image of Figure (3-2) shows the parallel display of a 2D Airy function pattern.

3.3 Tracing Amplitude Variation on the Image Plane

From Eq. (2-3-2), a fixed value on the β-axis leads to an Airy function by tracing the amplitude of the intensity. The amplitude tracing can be done by reading a row of the image matrix which holds data related to the intensity of a specific position. The location of the row to be measured is determined by the value of the simulation parameter analogous to the physical value of the spatial variable of the β-axis. The calibration factor between the simulation image and the physical diffraction pattern can be achieved from a comparison between the simulation parameter of a rectangular function with the theoretical parameter of the same function. It is calculated that 1 pixel of the image matrix corresponds to 0.041 mm of physical distance. (using $f = 680\,mm$, $\lambda = 632.8nm$)

Figure 3-3 is plotted based on the variation of intensity values on a row vector of Figure 3-2. The sampled row vector is located on the ninth pixel from the center of the output image.

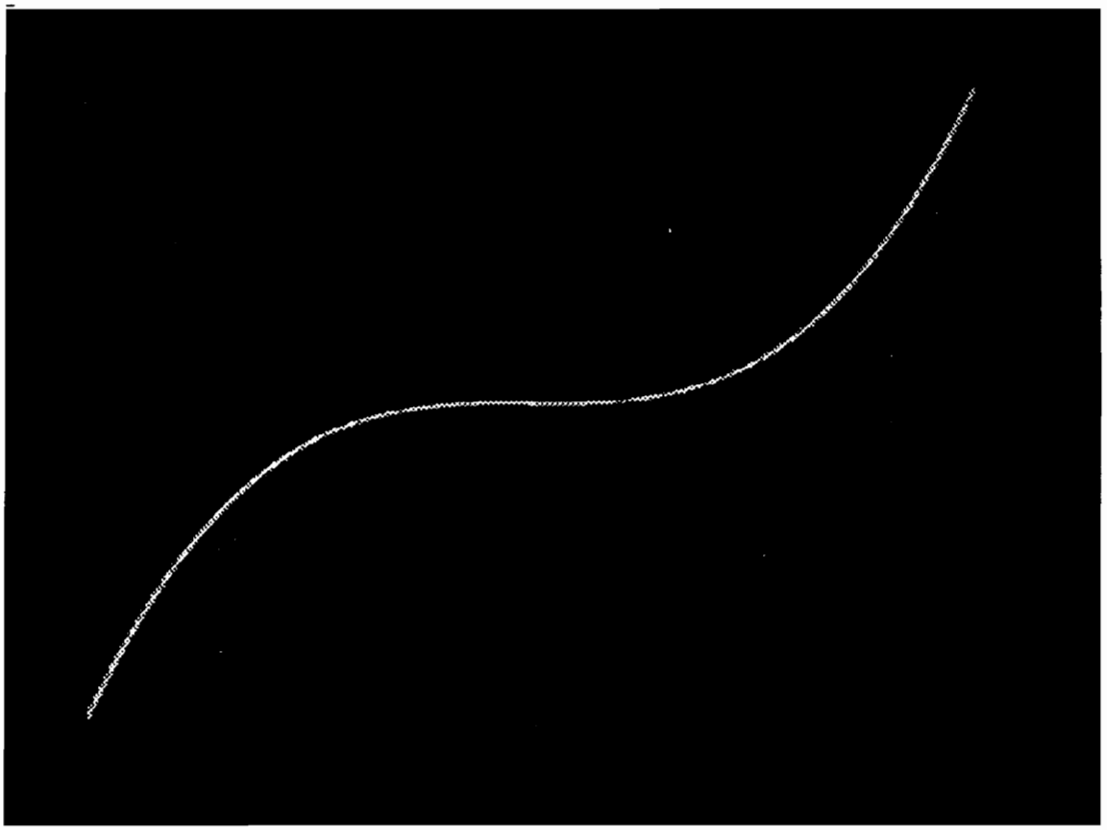

Figure 3-1 2D object matrix with the size of 512*512

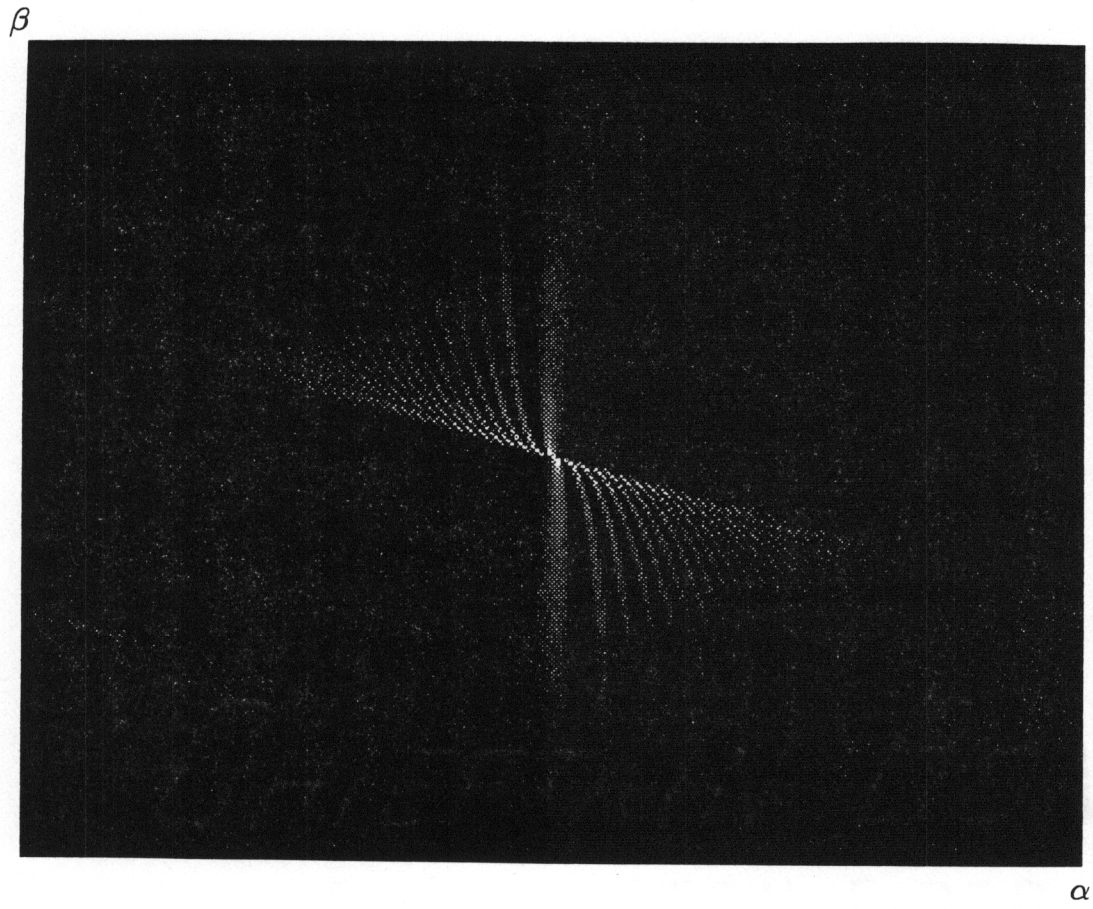

Figure 3-2 2D Fast Fourier transformed image matrix

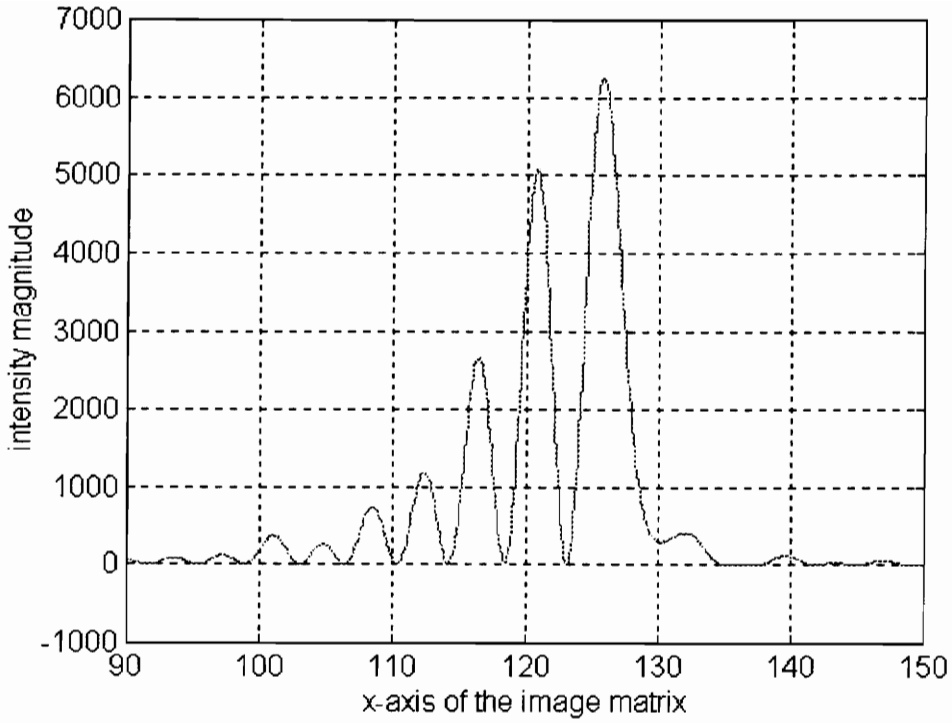

Figure 3-3 Intensity variation of a row vector from Figure 3-2

3.4 Effect of the Thickness of theTransparent Region

As mentioned in Eq. (3-1-1), the transparent region of the input amplitude transmittance should be represented by a Dirac delta function as follows:

$$T(x,y) = \delta(y - F(x)) \qquad . \tag{3-4-1}$$

The input function is given as $F(x) = \frac{1}{3}x^3$ and $T(x,y)$ is transparent only along the input function. However, the ideal condition for a Dirac delta function is not realized under the conditions of simulation (cf. Figure 3-1). In order to recognize the possible deviation caused in an actual simulation, it is needed to visualize the effect of the thickness of the high intensity region by having various input matrices with the different widths of $F(x)$. The width of $F(x)$ is controlled by applying a width-controlling function to the input matrix using a 2D-convolution. The width-controlling function can be produced in the form of a two-dimensional rectangular function as follows:

$$W(x,y) = \frac{1}{a^2} rect(\frac{x}{a}) rect(\frac{y}{a}). \tag{3-4-2}$$

Note that $rect(\frac{x}{a})$ represents a rectangular function with the width of a. The convolution of the equation (3-4-2) and the amplitude transmittance $T(x,y)$ becomes

$$T'(x,y) = T(x,y) * W(x,y)$$

$$= \delta(y - F(x)) * [\frac{1}{a^2} rect(\frac{x}{a}) rect(\frac{y}{a})]$$

$$= \frac{1}{a^2} \int rect(\frac{x-x'}{a}) rect(\frac{y-F(x')}{a})\, dx', \tag{3-4-3}$$

when '$*$' is the operator of convolution. The Fourier transformation pair of the convolution becomes

$$FT[\ T^{'}(x,y)\ ] = sinc(a\alpha)sinc(a\beta)FT[T(x,y)]$$

$$= sinc(a\alpha)sinc(a\beta)\{\int_{-\infty}^{\infty} exp(-j2\pi(\alpha x + \beta F(x)))dx\}, \text{(3-4-4)}$$

where $sinc(\gamma) = \frac{sin(\pi\gamma)}{\pi\gamma}$.

Figures of (3-4), (3-5) and (3-6) display the results with varying thickness. The widths of the rectangular functions applied are 4 pixels, 8 pixels and 15 pixels, respectively. It is shown that the intensity decreases faster for a fixed β and its variation loses the pattern of an Airy function as the function $F(x)$ gains thickness. This result can be anticipated from the fact that the first zero of *sinc* function is located closer to zero (the center of the image) as the thickness a increases. Furthermore, due to the low magnitude of the *sinc* function, the intensity value of the diffraction pattern decreases faster in the region of high spatial frequency.

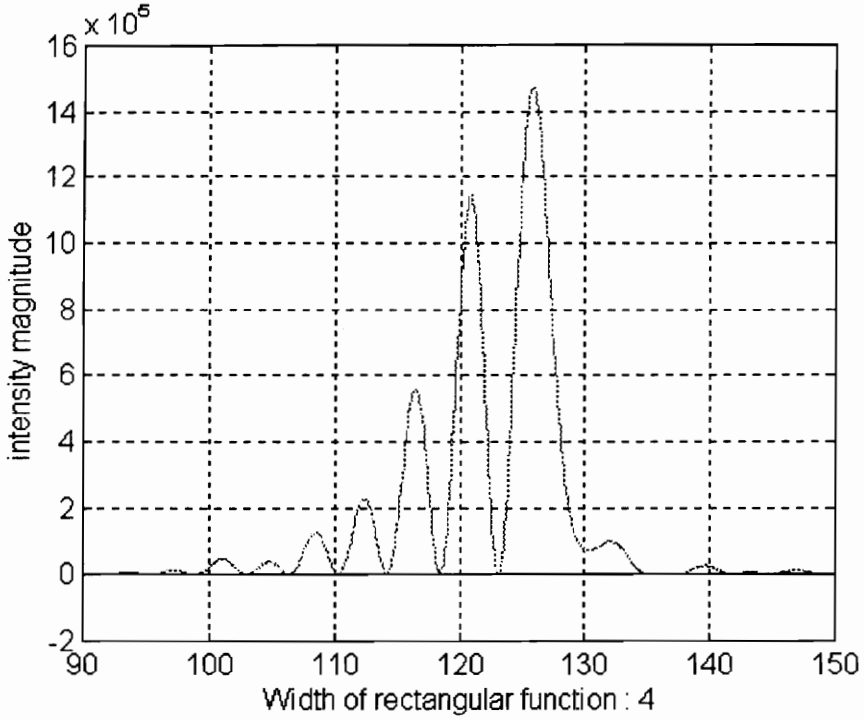

Figure 3-4. Sampled intensity variation on the10 th row vector from the center. (Width of applied rectangular function : 4 pixels)

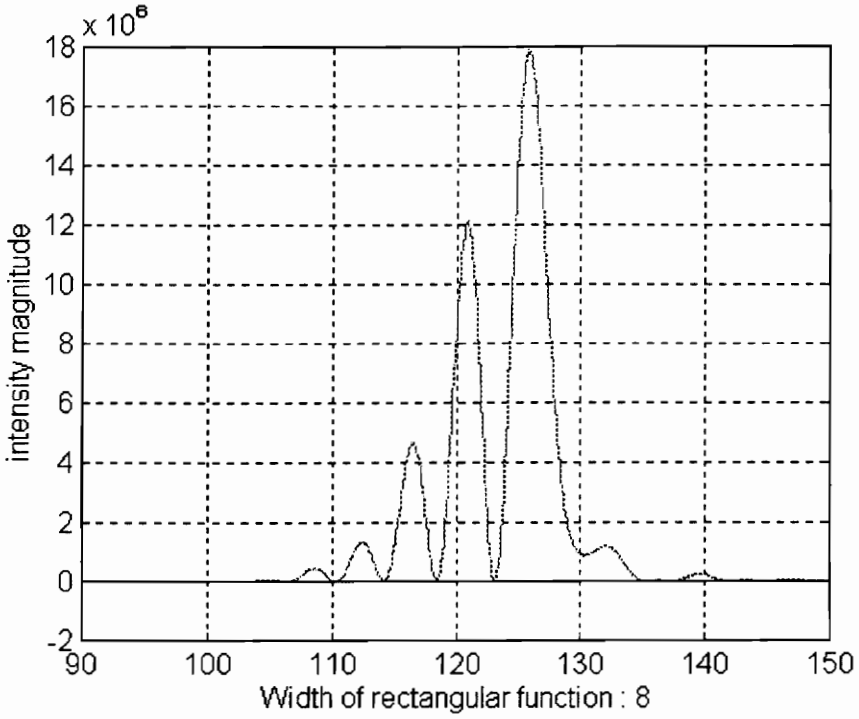

Figure 3-5. Sampled intensity variation on the10 th row vector from the center (Width of applied rectangular function : 8 pixels)

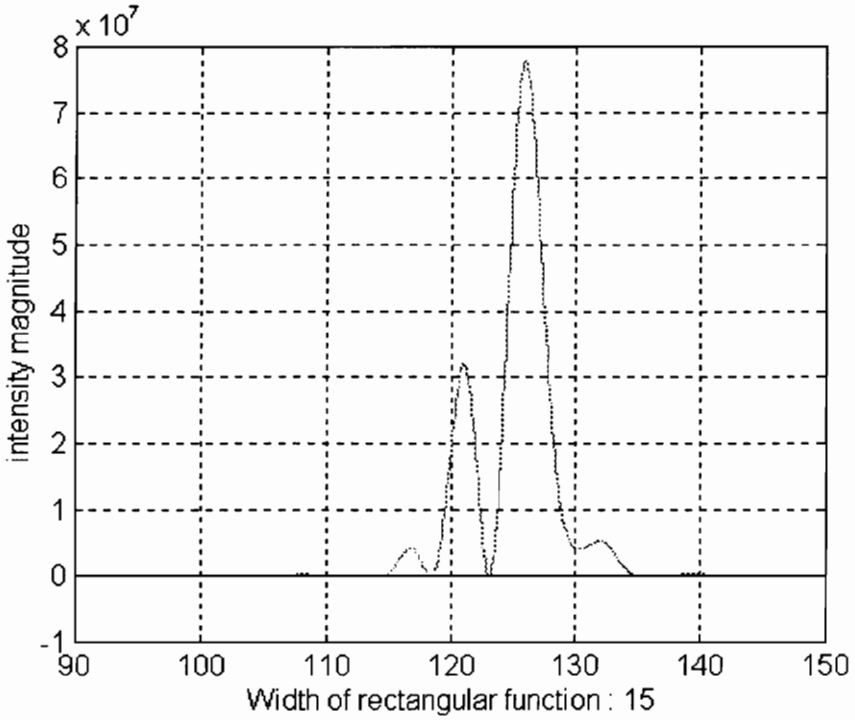

Figure 3-5. Sampled intensity variation on the10 th row vector from the center.(Width of applied rectangular function :15 pixels)

Chapter 4

OPTICAL EXPERIMENT

This experiment is conducted with two separate systems: **System A** for the observation of the diffraction pattern and **System B** for gathering the data of intensity variation. The output of System A and the data gathered from System B are presented in the next section, followed by the procedures for each experiment.

Similarly to the process of simulation, the optical experiment includes several fundamental procedures which are listed below:

* Creation of the 2D input object, which contains the intended function $F(x)$;
* 2D Fourier transformation of the input object by Fraunhofer diffraction using a lens system;
* Observation and detection of the intensity variation.

4.1 System A and Observation

Figure 4-1 shows the set-up for the observation of the diffraction pattern. The Fraunhofer diffraction pattern of the 2D input object is generated by a lens system. A spatial filter is placed in the path of laser to prevent the redundant area of $T(x, y)$ being processed. The diffraction pattern on the output image plane is observed by the monitor of a personal computer via a CCD camera. Based on the observed image pattern, the locations of intensity sampling devices are chosen prior to the intensity the measurement prior to the intensity

4.1.1 Input object

A photo-film containing the amplitude transmittance of the function to be processed was used as the two-dimensional input object of this optical experiment. The input object has the amplitude transmittance given in Eq. (2-3-1), and it needs to be transparent only along the function $F(x) = \frac{1}{3}x^3$, ideally. For consistency of the results, $T(x, y)$ is based on the 2D image matrix used in computer simulations. The dimensions of the object are 8 mm for each side, and $F(x)$ is transparent with a width of 0.2 mm (Fig. 4-2).

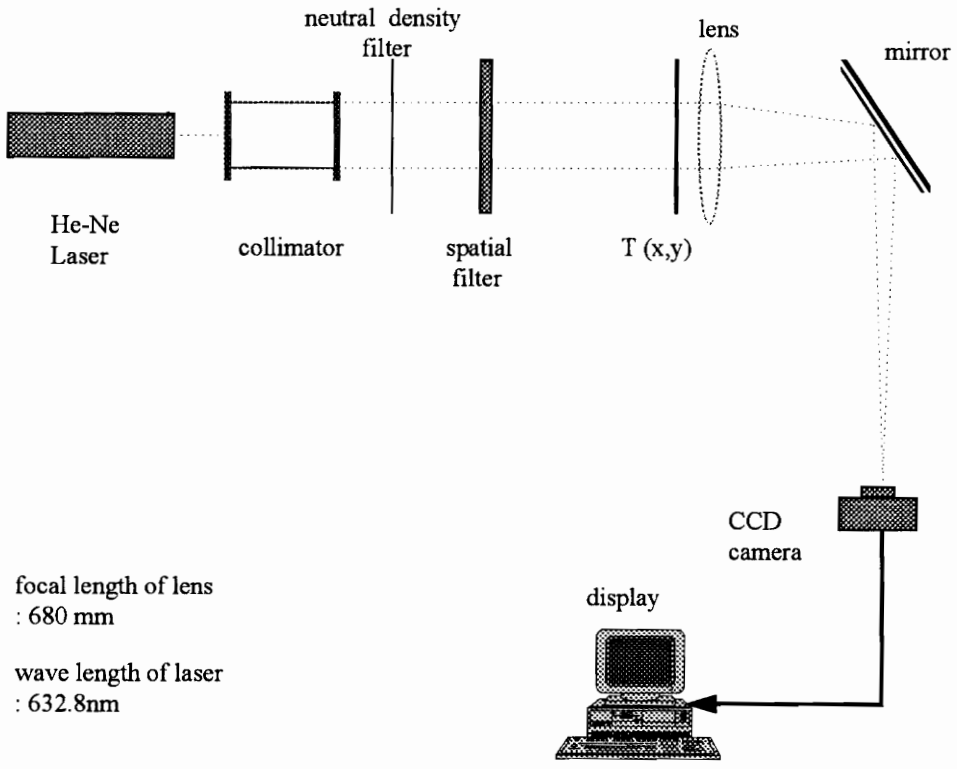

Figure 4-1 Optical set-up for the observation of the diffraction pattern

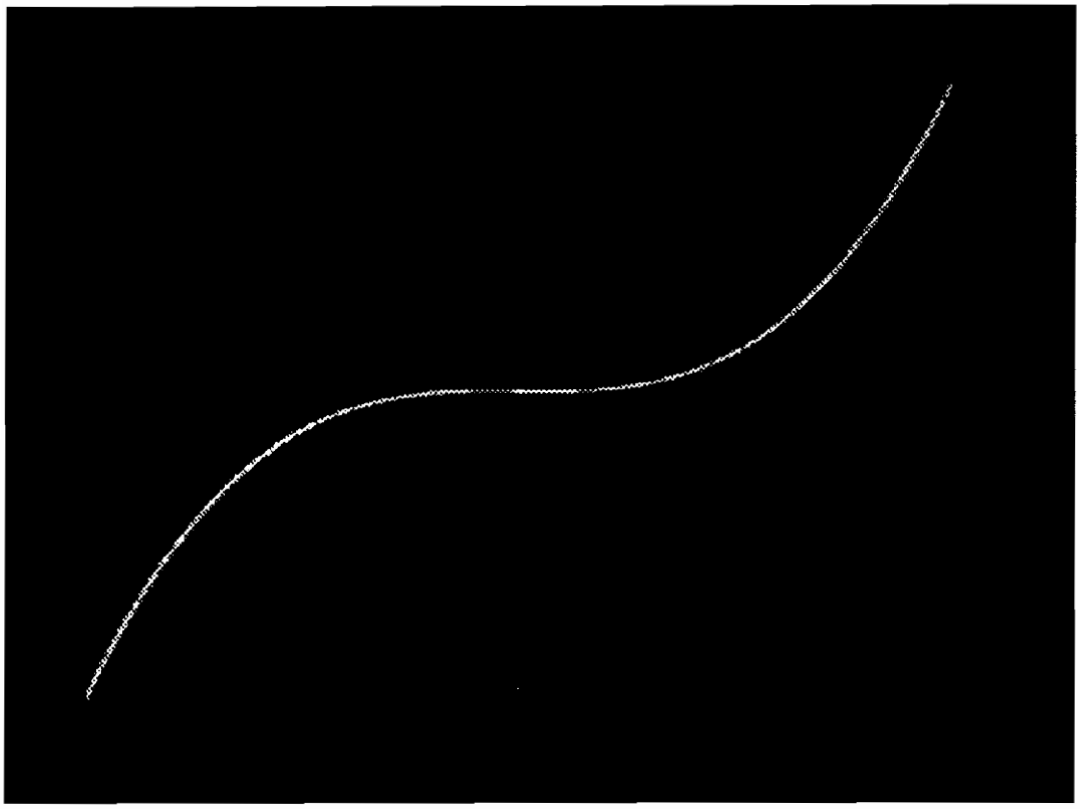

Figure 4-2 2D binary object of system A. (8 mm width for both sides)

4.1.2 Two-dimensional Fourier transform

Consider Figure 4-1. A plane wave emerging from a collimator with a wave length of λ=632.8 nm arrives at the lens plane. The light wave proceeds through $T(x, y)$ in front of the lens, and constructs an amplitude distribution proportional to the Fourier transform of the object $T(x, y)$ on the output image plane at which the CCD camera is located. A sampled image from the CCD camera is directed to a display unit. In order to obtain the image with the least amount of interference, the location of the camera is carefully adjusted and a filter (neutral density filter) is used in the path of the light wave to prevent excessive amount of light which causes saturation of the captured CCD image.

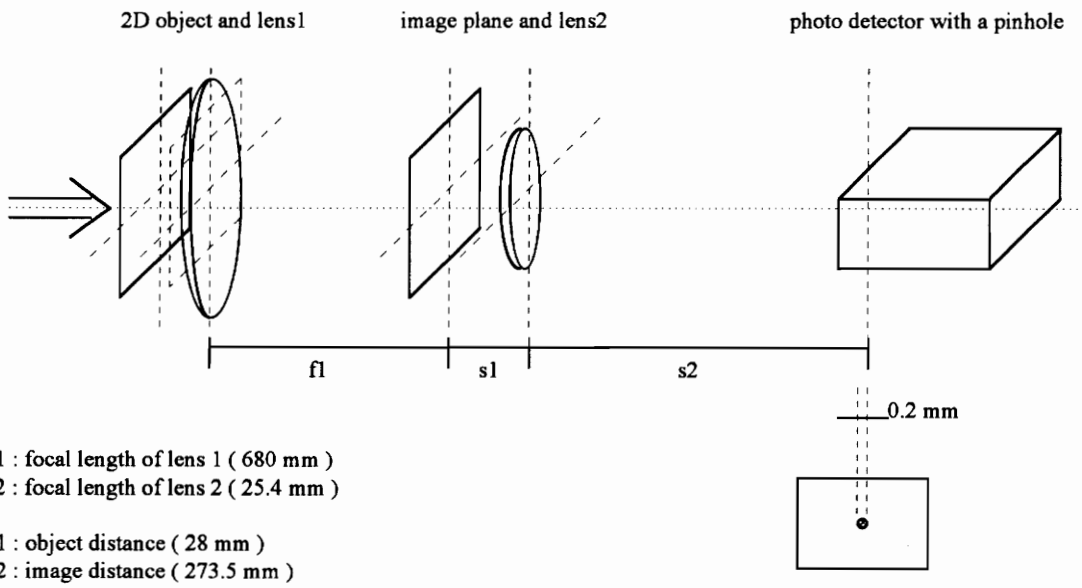

Figure 4-3 Optical set-up for intensity measurement

4.2 System B and Intensity Measurement

Figure 4-3 shows another experimental set-up, system B, which is for the sampling and measurement of resulting intensity. Notice that another lens, lens 2 ($f = 25.4\,mm$), is placed behind the back focal plane of lens1 to magnify the diffraction pattern. A photo-detector is placed on the image plane of the lens2 for the measurement of the intensity. In order to have more sampled points in a given range, a pin-hole (diameter of 0.2 mm) is placed in front of the photo-detector's input window. According to Eq. (2-3-2), a fixed value on the β-axis produces the Airy function with variable α. The value on the β-axis can be chosen by having the intensity measured on a horizontal line. The distance (τ) from the center of the output image to the location of the sampling line can be translated into the spatial variable on the β-axis by the relationship of $\omega = \frac{\tau}{\lambda f}$. Note that ω and f represent the spatial frequency and the focal length of the lens applied, receptively. The photo-detector is translated horizontally by a distance of a few millimeters for each movement. Meanwhile the intensity of the image is measured on each point of sampling. The output of the photo-detector is numerically visualized by a voltmeter and Table 4-1 shows the data read from the voltmeter and the relative distance of each sampling point. The measured intensity values are found to be fluctuating as the distance changes, while the overall intensity values are decreasing. The maximum intensity is measured at 1.4 (mV) on the first peak of the intensity. Based on the data of Table 4-1, Figure 4-5 of the intensity variation plot is constructed.

Table 4-1 Intensity variation of the diffraction pattern

(mm) Relative Distance	(mV) Intensity	(mm) Relative Distance	(mV) Intensity
7.92	0.0	4.25	0.45
7.75	0.1	4.10	0.00
7.5	0.4	4.00	0.20
7.25	0.9	3.75	0.65
7.0	1.3	3.6	0.30
6.83	**1.4** (max)	3.5	0.05
6.75	1.3	3.25	0.50
6.5	0.7	3.00	0.10
6.25	0.0	2.70	0.30
6.0	0.3	2.50	0.05
5.75	1.0	2.28	0.25
5.5	0.5	2.08	0.05
5.32	0.0	1.83	0.30
5.25	0.2	1.65	0.10
5.00	0.7	1.51	0.30
4.94	0.4	1.28	0.10
4.75	0.2	1.08	0.25
4.68	0.05	0.84	0.10
4.5	0.5	0.64	0.25
4.37	0.65	0.42	0.10

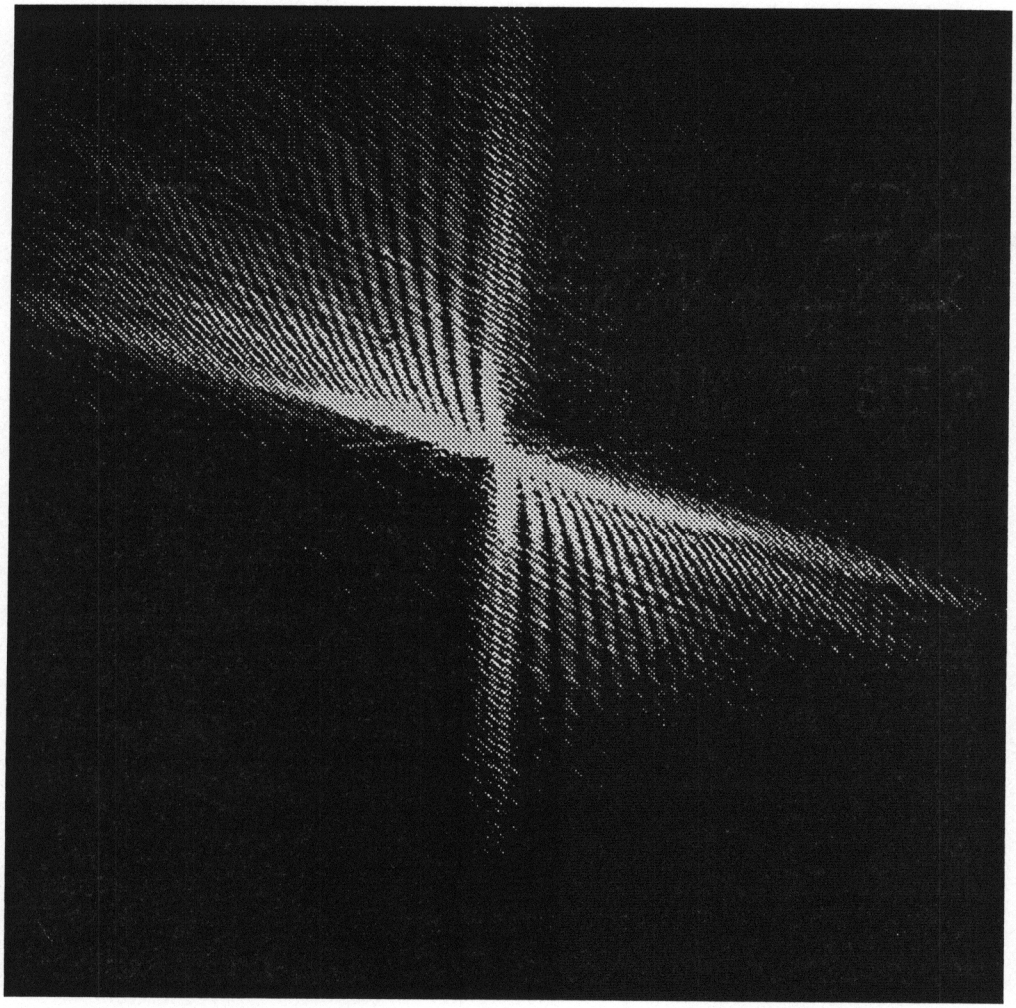

Figure 4-4 Optically produced Fraunhofer diffraction pattern of the 2D binary image.

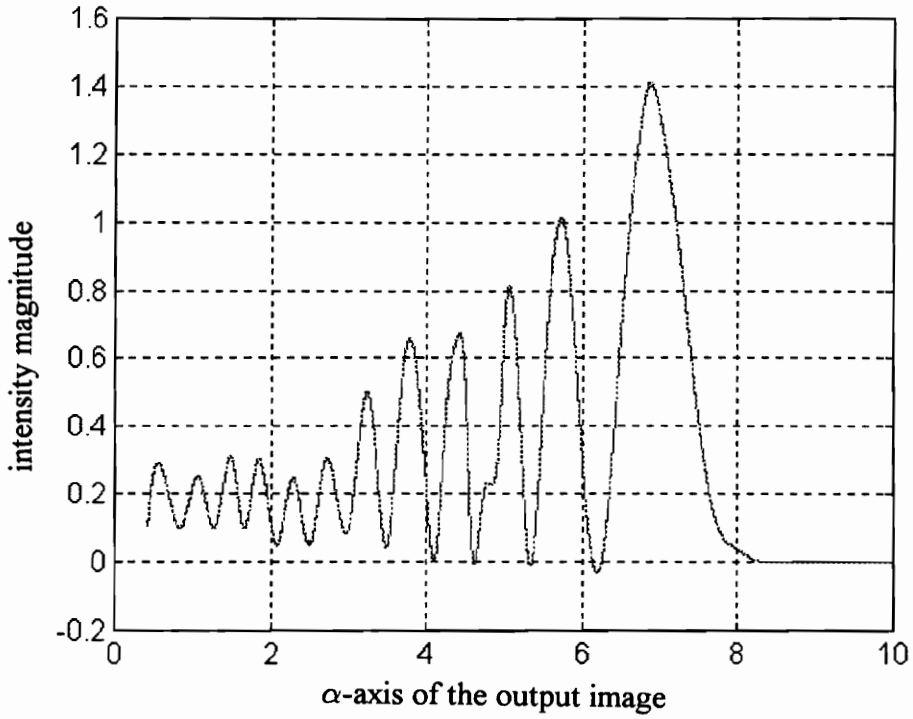

Figure 4-5 Intensity variation based on the data of Table 4-1.

4.3 Result from the Optical Set-up

4.3.1 Magnification of L_2

As mentioned in the experimental process, the data in Table 4-1 are from the magnified image. The magnification of the output image is determined by the focal length of the second lens, L2, and the distance between the image plane and L_2 (Figure 4-3). The lens formula is applied to calculate the magnification [6] [7], viz.,

$$\frac{1}{s_1} + \frac{1}{s_2} = \frac{1}{f}, \qquad (4\text{-}3\text{-}1)$$

where s_1 is the object distance, s_2 is the image distance, and f is the focal length of the magnifying lens L_2 (=24.5 mm). s_1 is measured at 2.60 cm and from the direct substitution of the given parameters in (4-3-1) we have

$$s_2 = \frac{2.60*2.45}{2.60-2.45} \simeq 42.47\, cm. \qquad (4\text{-}3\text{-}2)$$

The lateral magnification is then calculated as

$$|M| = \frac{s_2}{s_1} \simeq 16.33. \qquad (4\text{-}3\text{-}3)$$

Hence, the lens L_2 magnifies the output image by the factor of 16.33 with an image distance of 42.47 cm.

4.3.2 Generation of the Airy function based on parameters of the experiment.

The data in Table 4-1 are used to construct the intensity variation plot of Figure 4-5. In order to verify that the intensity plot represents the Airy function as it is anticipated, a qualitative comparison can be made with the theoretical function generated with parameters identical to those of the experiment. Equation (2-3-7) viz.,

$$I(\alpha,\omega) = \{2\pi(6\pi c\beta)^{-\frac{1}{3}}\}^2[\,Ai\{(6\pi c\beta)^{-\frac{1}{3}}2\pi\alpha\}]^2\,|_{\beta=\omega,} \qquad (4\text{-}3\text{-}4)$$

provides the theoretical representation of the intensity sampled from the parallel display of the 2D Airy function Fraunhofer diffraction pattern. This expression includes an arbitrary constant c, the location of horizontal sampling w, the spatial frequency variable α, and the wavelength λ=632.8 nm. From the experiment, the distance τ from the center of the output image to the location of the sampled horizontal line is measured at 38 mm. Considering the magnification factor of the image, the actual distance τ can be calculated as $\tau = \frac{38}{|M|} = \frac{38}{16.33} \simeq 2.33$ mm. Given the wavelength λ=632.8 nm, the spatial frequency variable ω is calculated as follows:

$$\omega = \frac{\tau}{\lambda f} = \frac{2.33}{632.8*10^{-6}*(680)} \simeq 5.41\,mm^{-1}. \qquad (4\text{-}3\text{-}5)$$

The relative distance τ, incorporated in the data given in Table 4-1, can be translated into the spatial frequency α using an expression analogous to that given in Eq. (4-3-5). Substituting the values of α, c and w into equation (4-3-4), an Airy function is generated. A qualitative comparison between the normalized intensity variations of Figure 4-5 and the theoretically generated Airy function can be seen in Figure 4-6.

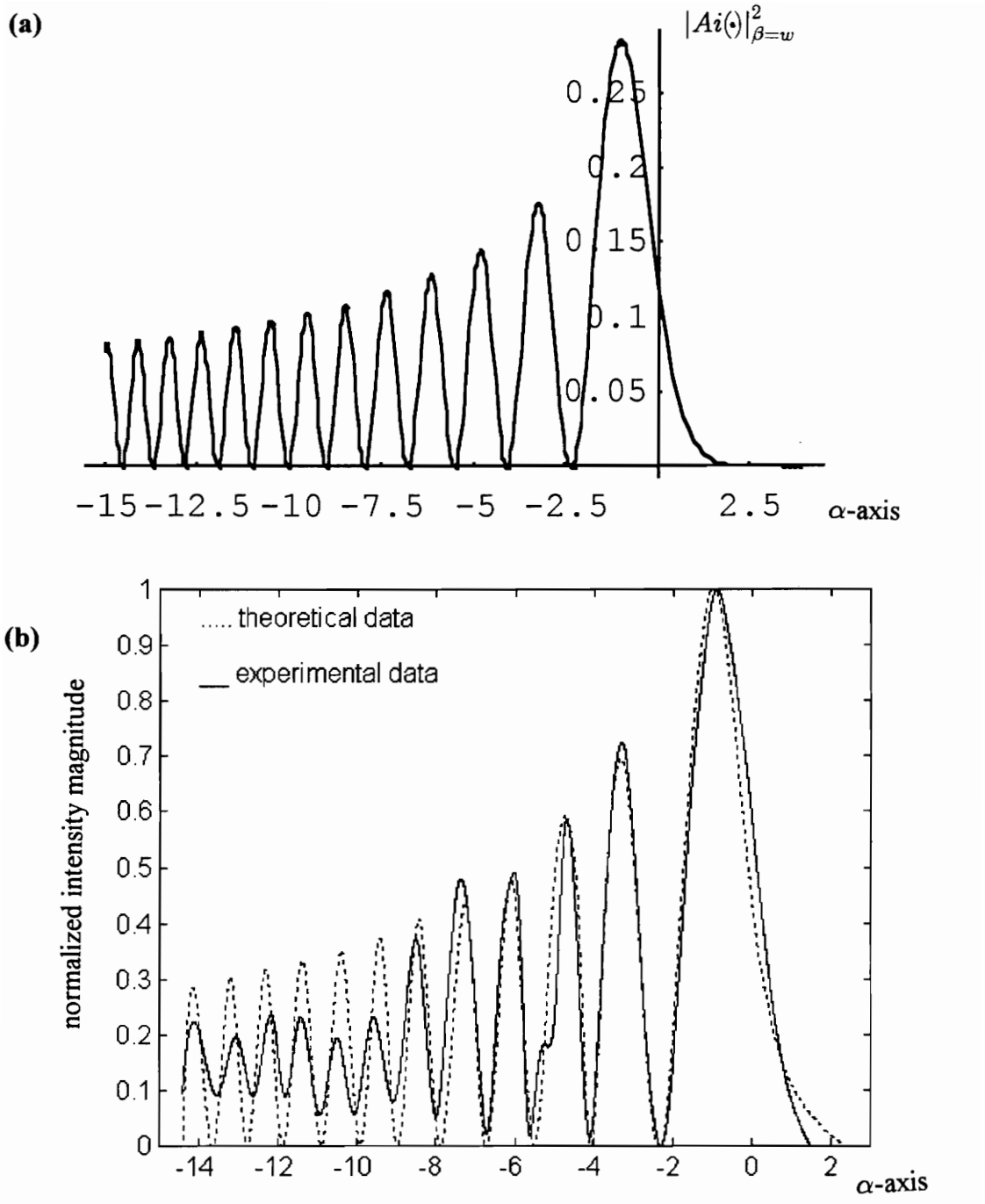

Figure 4-6 (a) Airy function constructed theoretically on the basis of the experimental parameters. (b) Qualitative comparison of Figure 4-5 and 4-6a

4.4 Discussion of the Output

It is appropriate at this stage to discuss the deviation of the experimental results from the theoretical values (Figure 4-6b). Based on the simulations and the procedures of the experiment, there are two main sources causing these deviations: 1) the thickness of the transparent region in the amplitude transmittance and 2) the noise coming from experimental environment.

4.4.1 Error due to the thickness of the transparent region

As pointed out earlier, the 2D actual object mask does not have the amplitude transmittance $T(x,y) = \delta[y - F(x)]$ that represents ideally a Dirac delta function. Suppose we use, instead, the amplitude transmittance $T'(x,y)$ discussed in Ch. 3, viz., the convolution of the ideal amplitude transmittance $T(x,y)$ with a rectangular function $W(x,y) = \frac{1}{a^2} rect(\frac{x}{a}) rect(\frac{y}{a})$. The 2D Fourier transform of $T'(x,y)$ given in Eq. (3-4-4) suggests that the thickness of the input object can cause errors in the output image by creating unwanted amplitude attenuation due to the two-dimensional *sinc* function multiplying the ideal diffraction pattern.

The simulation results discussed in Chapter 3 support the fact that increasing the thickness of the transparent region causes a higher degree of deviation compared with the theoretical results. The intensity decreases faster as it approaches a higher spatial frequency region.

4.4.2 Noise from the characteristic properties of the light wave

Figures 4-6a and 4-6b show that the intensity values in the experimental data decrease faster than those of 4-6a as the observation point goes farther from the center of

the image. In the high spatial frequency region, the measured intensity was sometimes low and, hence, outside the range of accurate measurement.

Another source of error is that the light wave used was not an ideal plane wave, even after collimation. The Gaussian property of the actual light wave also can cause a faster decrease of the intensity value as the distance from the center gets larger.

Chapter 5

OPTICAL DISPLAY OF PROPAGATION OF A TRANSIENT WAVE IN A DISPERSIVE MEDIUM

In the previous chapter we optically displayed an Airy function. Using the same method we would like to show that the one-dimensional space-time evolution of a wave packet in a dispersive medium can be optically displayed. Starting with the Fourier description of one-dimensional transient wave propagation in a dispersive medium, our discussion involves the scheme of the optical experiment and the simulation results.

5.1 Transient Wave Propagation in a Dispersive Medium

For many classes of dispersive systems, the wave function $\psi(\underline{x}\,, t)$ is given by the Fourier integral [17, 18]

$$\psi(\underline{x}\,, t) = \tfrac{1}{2\pi}\int_{R^3} exp[j(\underline{k}\cdot\underline{x} - \Omega(\underline{k})t]\Psi_o(\underline{k})d\underline{k}, \qquad t > 0 \qquad (5\text{-}1\text{-}1)$$

$$\psi(\underline{x}\,, 0) = \psi_o(\underline{x}). \qquad (5\text{-}1\text{-}2)$$

$\omega = \Omega(\underline{k})$ is the three dimensional dispersion relationship between the angular frequency w and the wave vector k. $\Psi_o(k)$ denotes the initial $(t = 0)$ spectrum of the signal $\psi(\underline{x}\,, t)$.

Without loss of generality, a one-dimensional version of equation (5-1-1) with single mode of the dispersion relationship of $w = \Omega(k)$ is given as [17][18]

$$\psi(x\,, t) = \tfrac{1}{2\pi}\int_{-\infty}^{\infty} exp[j(kx - \Omega(k)t]\Psi_o(k)dk, \quad t > 0. \qquad (5\text{-}1\text{-}3)$$

Let us consider specifically the dispersion relation

$$\Omega(k) = -\frac{k^3}{3}, \tag{5-1-4}$$

while the initial spectrum is given as

$$\Psi_o(k) = \sqrt{2\pi}exp[-\frac{k^2}{2}]. \tag{5-1-5}$$

Substitution of (5-1-4) and (5-1-5) into (5-1-3) results in the wave field

$$\psi(x\,,t) = \frac{1}{\sqrt{2\pi}}\int_{-\infty}^{\infty} exp[j(kx + \frac{k^3}{3}t) - \frac{k^2}{2}]dk. \tag{5-1-6}$$

The integration of equation (5-1-6) can be carried out explicitly [17], yielding the wave field

$$\psi(x\,,t) = \sqrt{2\pi}\,t^{-\frac{1}{3}} exp\{\frac{1}{2t}(x + \frac{1}{6t})\}Ai\{t^{-\frac{1}{3}}[x + \frac{1}{4t}]\}, \tag{5-1-7}$$

where $Ai(\,)$ is an Airy function.

Consider, next, the Fraunhofer diffraction pattern produced from an input transparency which has the amplitude transmittance

$$T(x,y) = h(x)\delta(y + F(x)), \tag{5-1-8}$$

where $h(x)$ is the amplitude transmittance of a binary mask located immediately in front of another 2D-binary mask as in Figure 5-1. From equation (2-2-4), the object masks generate the Fraunhofer diffraction pattern

$$U_f(\alpha,\beta) = \frac{exp(jkf)}{j\lambda f} exp[j\lambda f\pi(\alpha^2+\beta^2)]\int_{-\infty}^{\infty} h(x) exp[j2\pi(x\alpha - \beta F(x))]dx, \tag{5-1-9}$$

whose intensity is given by

$$|U_f(\alpha,\beta)|^2 = (\frac{1}{\lambda f})^2 |\int_{-\infty}^{\infty} h(x) exp[j2\pi(x\alpha - \beta F(x))]dx|^2. \tag{5-1-10}$$

Comparing equation (5-1-10) with the intensity of the wave field given in Eq. (5-1-3) suggests the following analogies

$2\pi\alpha$	<---------->	x
$2\pi\beta$	<---------->	t
$F(x)$	<---------->	$\Omega(k)$
x	<---------->	k
$h(x)$	<---------->	$\Psi_o(k)$

Thus, it is feasible to display the space-time evolution of a transient wave packet propagating in a dispersive medium by the optical method. From equation (5-1-8) and the analogy above, it is seen that two juxtaposed two-dimensional masks are required for the optical experiment. One mask contains information about the dispersion relation ($\Omega(k)$) and the other about the spatial spectrum of the initial pulse ($\Psi_o(k)$). Since an intensity sampling line at β=ω is analogous to a fixed time, one would be able to observe the time-

space evolution of the wave packet by varying ω. Based on equation (5-1-7), choosing $F(x) = -\frac{x^3}{3}$ and $h(x) = \sqrt{2\pi}exp[-\frac{x^2}{2}]$ would yield

$$I(\alpha,\beta)|_{\beta=\omega} = \frac{4\pi^2}{(\lambda f)^2}|\sqrt{2\pi}w^{-\frac{1}{3}}exp\{\frac{1}{2w}(\alpha+\frac{1}{6w})\}Ai\{w^{-\frac{1}{3}}[\alpha+\frac{1}{4w}]\}|^2, \qquad (5\text{-}1\text{-}11)$$

where $I(\alpha,\beta)$ denotes the intensity of the displayed pattern.

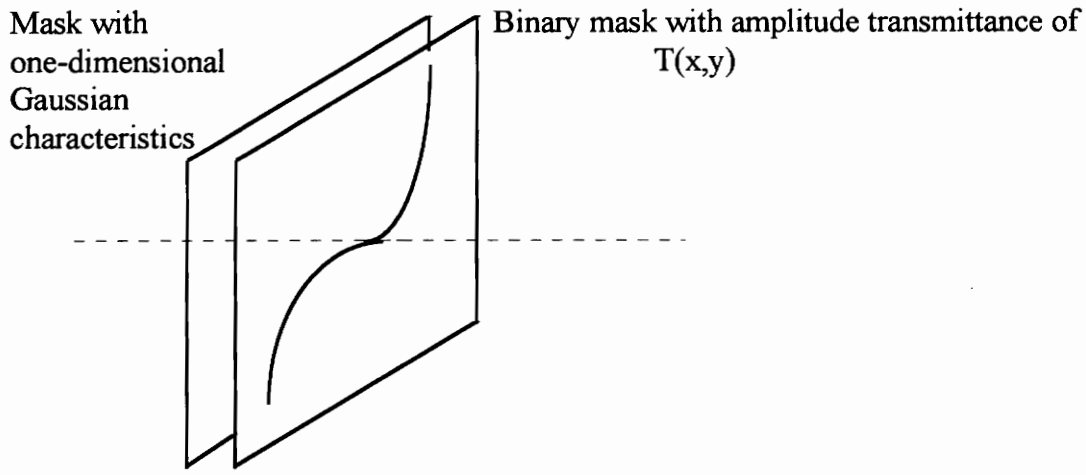

Figure 5-1 Two juxtaposed masks containing the information about the dispersive relation ($T(x, y)$) and the spatial spectrum of the transient wave propagating in a dispersive medium.

5.2 Simulation of Transient Wave Propagation in a Dispersive Medium

As Figure 5-1 of the optical set-up indicates, two object matrices are required for a computer simulation. In this case, one matrix needs to contain information about the dispersion relation while the other has to specify the initial spectrum. Again, the input transparency and the output image of the computer simulations are assigned as input and output matrices. On the basis of the theoretical analysis of the previous section, we choose

$$F(x) = -\frac{1}{3}x^3, \tag{5-2-1}$$

and

$$h(x) = \sqrt{2\pi}exp[-\frac{x^2}{2}]. \tag{5-2-2}$$

The binary input matrix with amplitude transmittance $T_{dispersion}(x, y) = \delta(y - \frac{1}{3}x^3)$ is constructed by the same procedure as the one discussed in Chapter 3. We call it Input Matrix A. The one-dimensional Gaussian function $h(x)$ generates another object. (see the code in Appendix A) and it is called Input Matrix B. Based on the Eq. (5-1-9), the Input Matrix A and the Input Matrix B are 2D-Fourier transformed after they are multiplied by each other. The resulting Fraunhofer diffraction pattern is shown in Figure 5-2.

Remember that the time variable t is analogous to $2\pi\beta$. In other words, the location of an intensity sampling line on the β-axis of the diffraction pattern of Figure 5-2 has an analogous value to the time variable. Figures 5-3abc show the horizontally sampled intensity variation of the resulting image matrix for various values of β from the center of

the matrix. In the environment of the experimental set-up, the location of the horizontal sampling line can be calibrated from the simulation image matrix to the physical value of $2\pi\beta$. From a simple derivation based on FFT2 of a rectangular function, the calibration constant is calculated to be 1 pixel=0.041 mm. As an example, from Figure 5-2b a horizontal sampling line is chosen to be the 13th pixel vector from the center of the image matrix. The physical value of τ is calculated to be 13*0.041=0.533 mm, while the time variable is analogous to $2\pi\beta = 2\pi\frac{\tau}{\lambda f}$.

Figures 5-3abc show the intensity variation patterns resulting from the simulations. Figure 5-3a has the sampling line located at the center of the image, while Figure 5-3b and Figure 5-3c are sampled from 13th and 28th row vectors, respectively, from the center. Changing sampling locations creates the changes of the intensity variation pattern, (Figure 5-3d) which implies the space-time evolution of the wave packet in the dispersive medium. Figure 5-3d is the overlap plotting of Figure 5-3a to 5-3c. The intensity patterns qualitatively follow the theoretical expectation constructed by Sockell. [17]

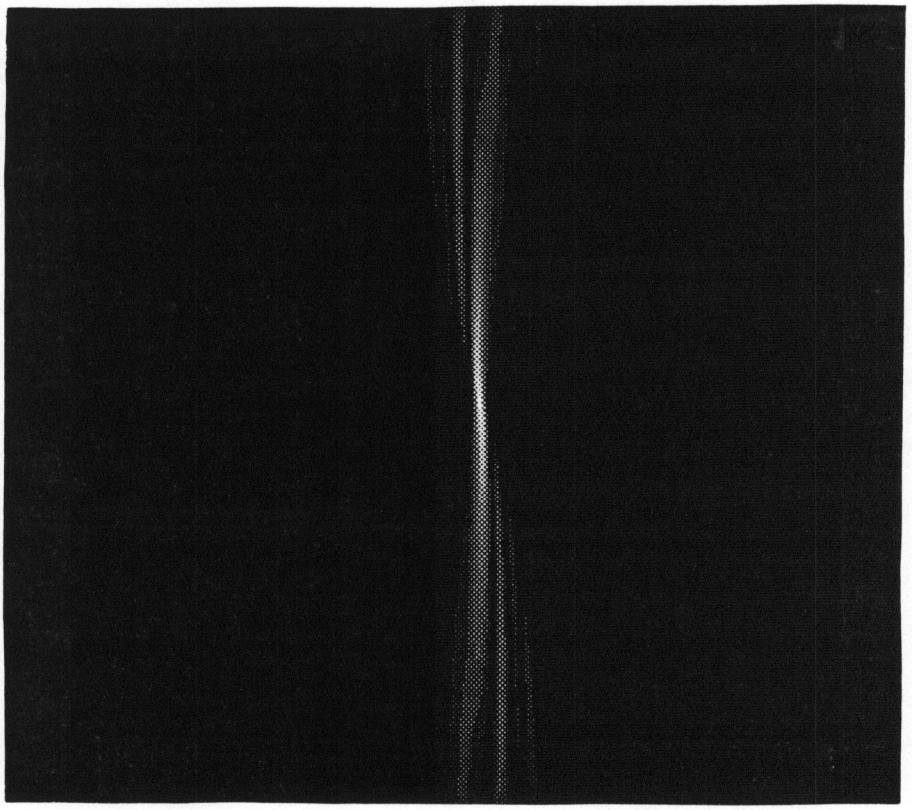

Figure 5-2 Result of 2D FFT of object with 1D Gaussian function

(a)

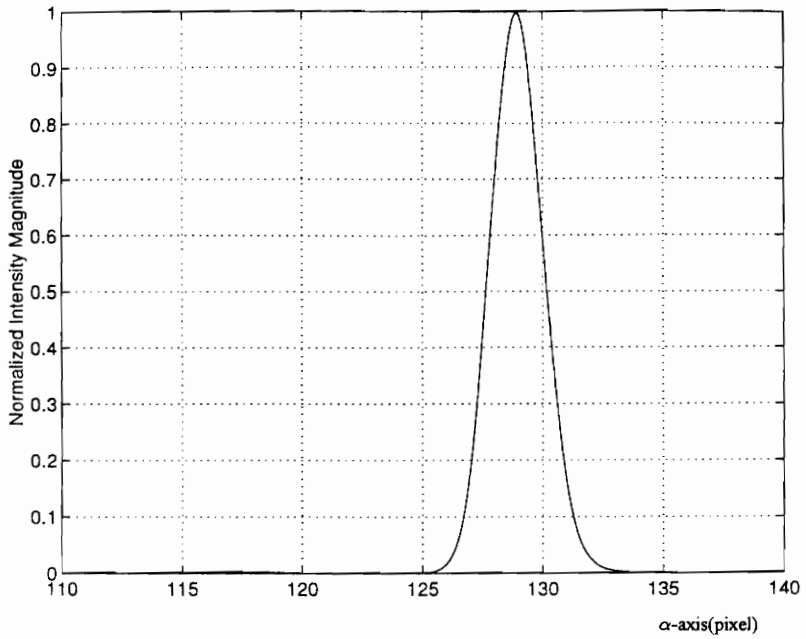

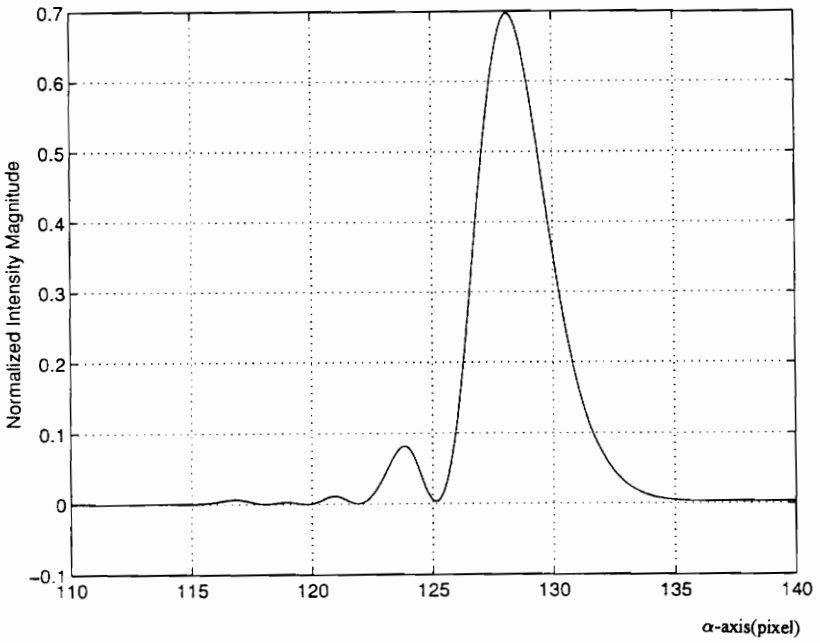

(b)

Figure 5-3a. Intensity variation from the row vector located at the center of the image.

b. Intensity variation of the 13th row vector from the center of the image

(c)

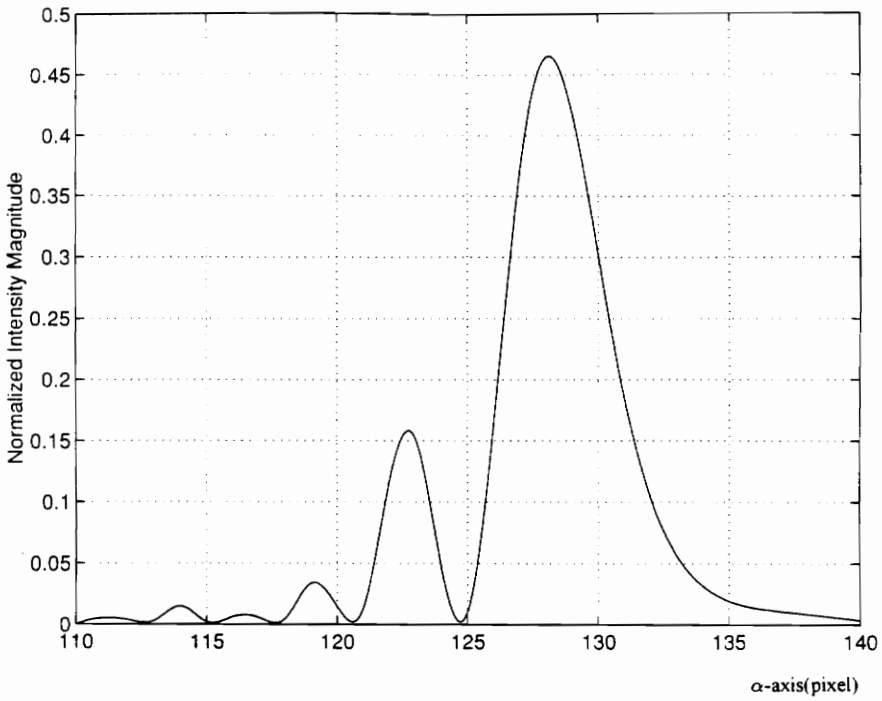

Figure 5-3c. Intensity variation of the 28th row vector from the center of the image

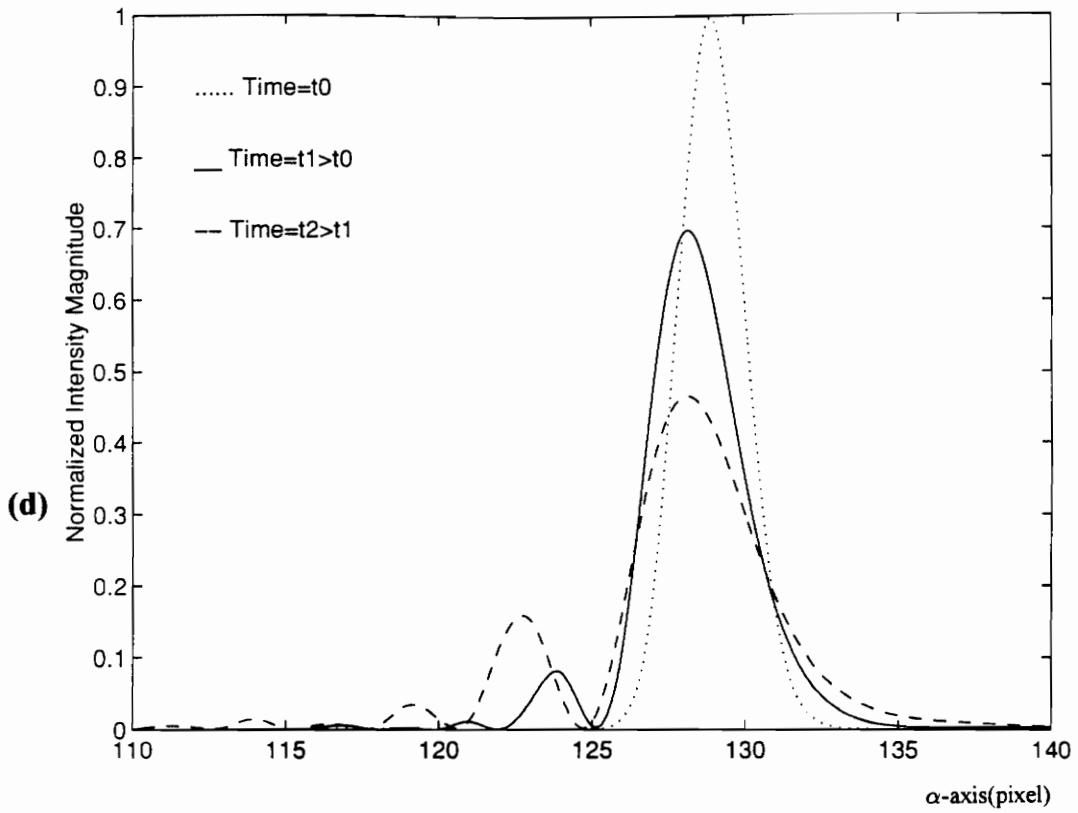

Figure 5-3d Normalized intensity variation patterns of different time constant. (by different sampling locations)

Chapter 6

OPTICAL PROCESSING USING AN EBSLM

Photo-films are not suitable as object masks for optical experiments requiring the multiplication of two or more object masks in real time. A Spatial Light Modulator (SLM) may produce a two-dimensional image that can be processed as the object mask of the optical experiment. The adaptation of a SLM makes it more controllable to generate desired 2D objects by using a personal computer.

Figure 6-1 shows the experimental apparatus containing an Electron Beam Addressed Spatial Light Modulator (EBSLM). The desired amplitude transmittance of the object mask is created by a personal computer and sent to the EBSLM controller in the form of a series of video signals. The EBSLM controller directs the signal to an electron gun and deflection coils which are located in the EBSLM head. The electron gun emits electrons in the modulated pattern by the input signal. At the end of the electron beam, a $LiNbO_3$ crystal accumulates the emitted charges. Deflecting coils generate a magnetic field which controls electrons and, hence, enables scanning the target crystal two-dimensionally. The refractive index of the surface of the crystal is changed by an electro-optic effect created by the accumulated electron charge. [19][20][21]

By illuminating the crystal with a linearly polarized laser, the charge pattern on the crystal can be read. The output read from the crystal is an elliptical polarized light and this light can be converted into a coherent image by passing it through an analyzer. The image after the analyzer is spatially filtered to remove the noise present in the high spatial frequency region. The resulting image projected onto a lens is processed to generate a Fraunhofer diffraction pattern. Using a photo-detector with a pin-hole, the intensity pattern of the diffraction pattern can be measured.

An input 2D-object of the EBSLM was generated based on that of the experiment in Chapter 4, using a personal computer. Figure 6-2 shows the input created by the computer. Figure 6-3 shows the resulting diffraction pattern on the image plane of the optical set-up. Even though the image on the output plane was close to the result that we expected from previous experiments, there were several aspects indicating that the image pattern did not have the intensity required for the observation and measurement of the intensity variation.

EBSLM requires a broadly collimated reference beam for the readout of the output charge pattern from the crystal. With a given laser input, the intensity of the reference beam becomes lower as the beam covers a large area and, as expected, the object (mask) read from EBSLM has low intensity. As the object is being processed through the optical set-up, the output pattern needs to be magnified in order for the photo-detector to read the variation of the intensity amplitude. The magnification of the image pattern also results in a lower intensity. High precision operational amplifiers are applied to compensate for the loss of the intensity, but the incoming signals to the amplifiers are heavily affected by noise and the magnified image pattern loses the characteristics of the desired image pattern. [22] Due to the damage on the magnified output image, the data of the intensity pattern has been constructed only by the computer readings of CCD instead of intensity measurement using the photo-detector. Figure 6-4 shows the constructed intensity variation from the diffraction pattern of Figure 6-3. The fluctuating intensity and decreasing overall magnitude of Figure 6-4 can be compared to the patterns of the simulated results, Figure 5-3d, however, when the location of the sampling (8th pixel) and the unexpected variation patterns are taken into account Figure 6-4 does not show the effect of gaussian characteristics applied nor the output with desirable quality.

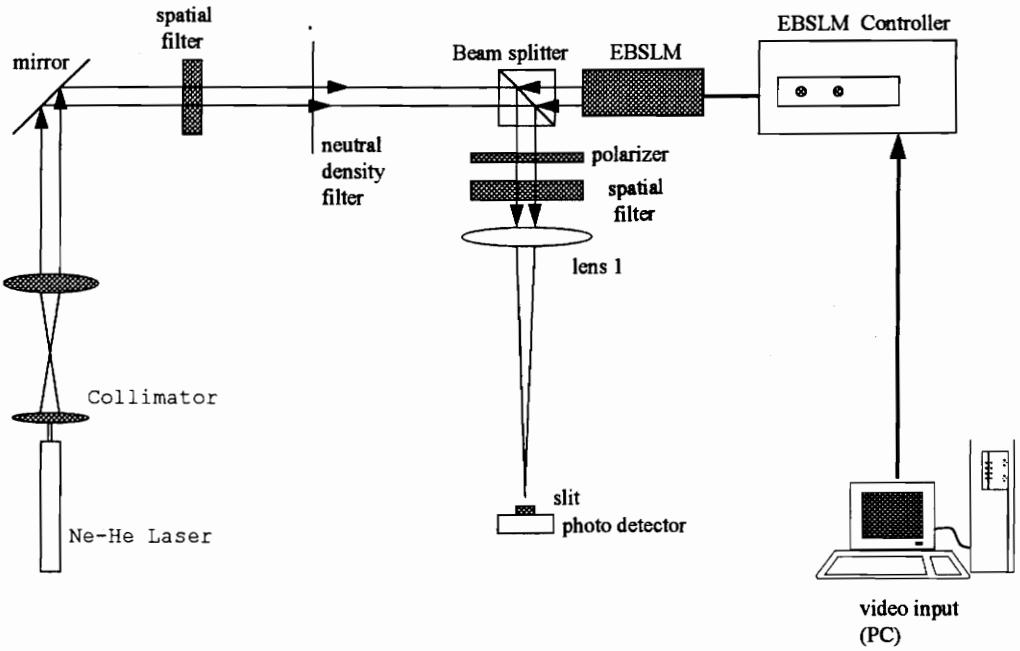

Figure 6-1. Set-up using an EBSLM

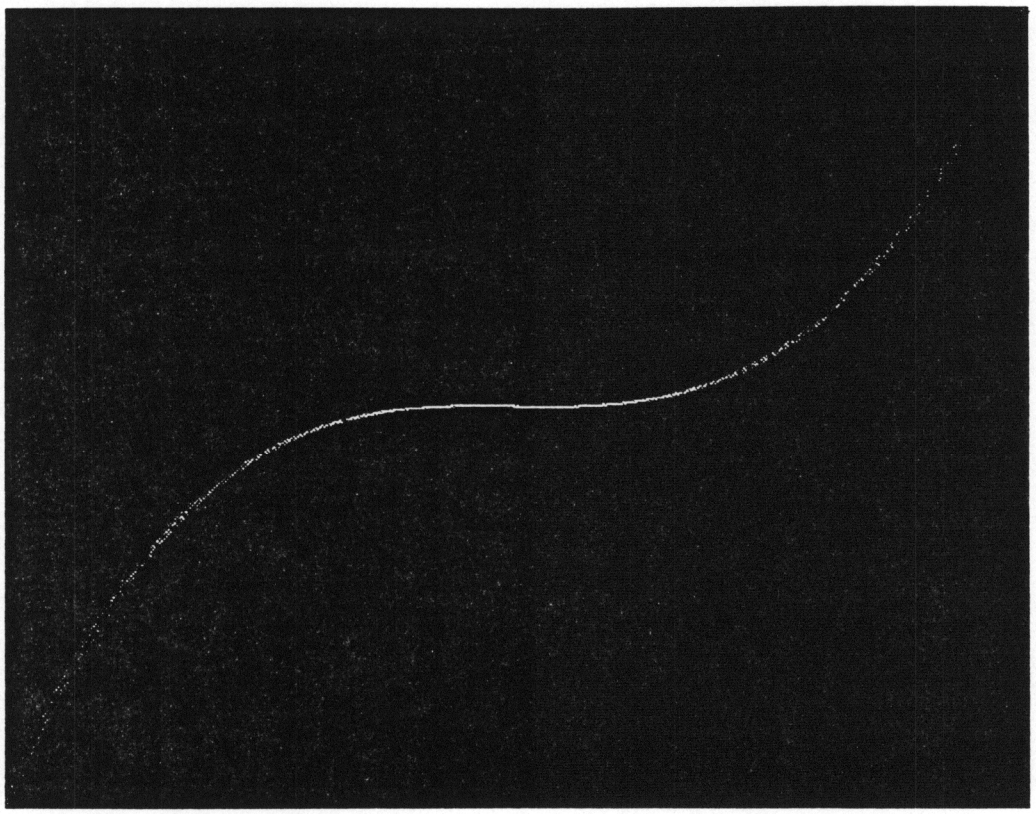

Figure 6-2. EBSLM input amplitude transmittance

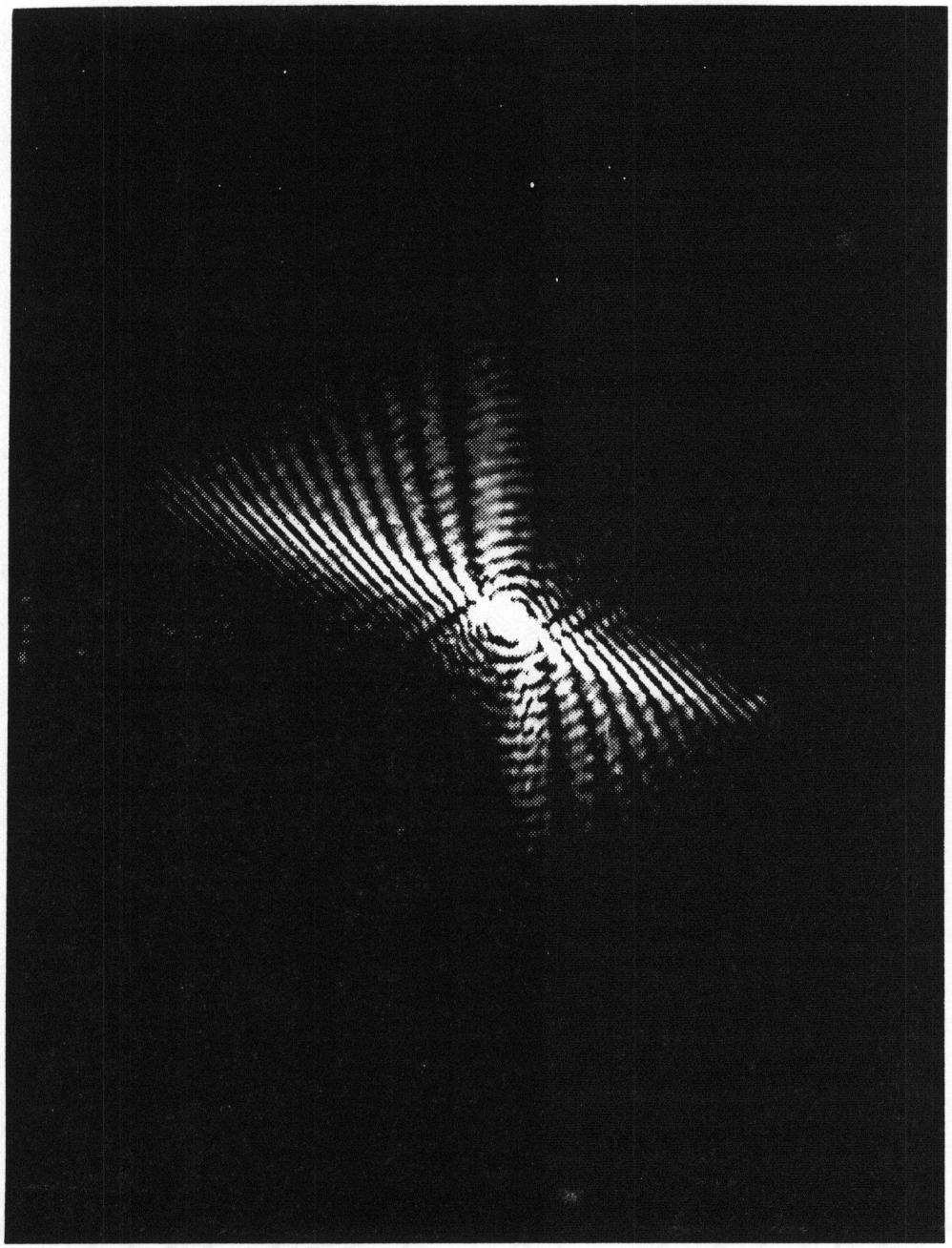

Figure 6-3. Diffraction pattern of the 2D object from an EBSLM

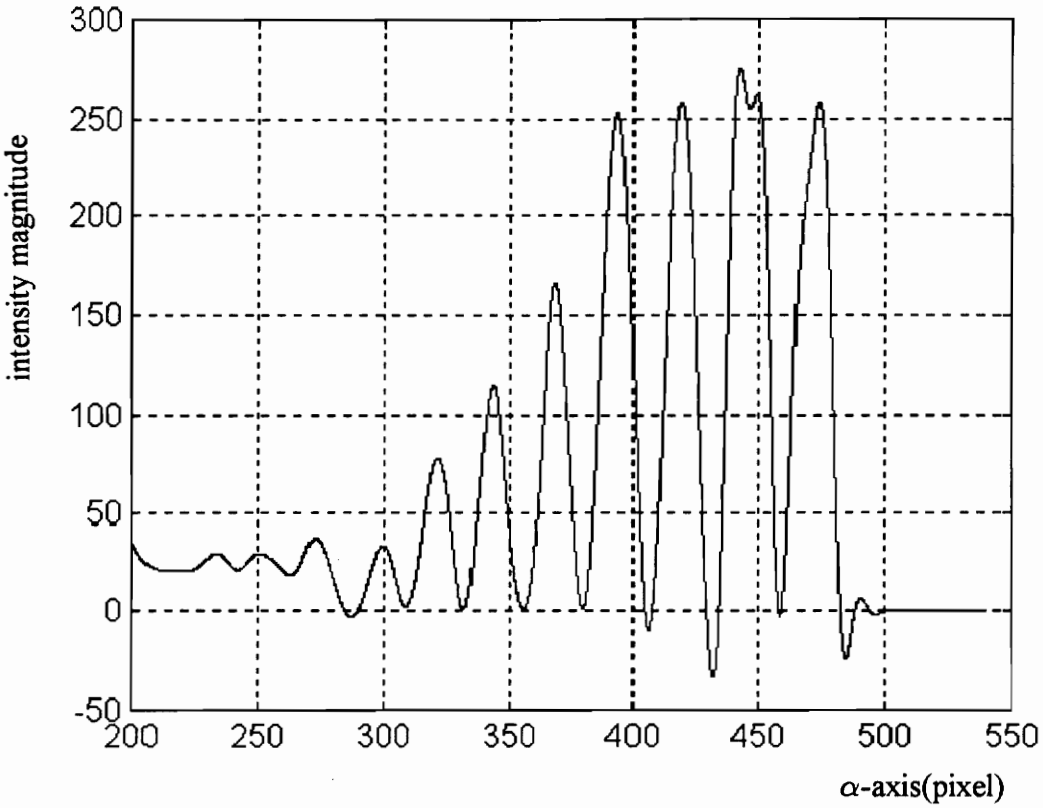

Figure 6-4. Intensity variation of figure 6-3, created by Computer reading of CCD image.

Chapter 7

CONCLUSION

7.1 Summary

An optical display of the Airy function has been demonstrated along with an application of the optical display technique to transient wave propagation in a dispersive medium. For the formation of optical Fourier transformation, a lens system is employed based on the Fresnel diffraction theory. A set of simulations are performed prior to the experiments and they provide estimated results corresponding to various parameter changes. Experimental results are given for the intensity measurement of the output images of the lens system. The variation of the measured intensity is analyzed and compared with the theoretically anticipated values.

The space-time evolution of a transient wave in a dispersive medium is proposed to be optically displayed, as an application of the optical display method. Based upon the theoretical analogy in Chapter 5, the Fourier description of one-dimensional transient wave propagation in a dispersive medium is found to be analogous to the equation achieved from the optical Fourier transformer. A simulation is added to the theoretical analysis, and it is followed by an experimental attempt using a Spatial Light Modulator (SLM). The 2D image generated by the SLM replaces the object mask of the optical set-up. When the advantage of manipulation of the amplitude transmittance is taken into account, the optical system with the SLM makes it easier to generate a complicated input amplitude transmittance which usually requires two or more object masks. It is, however, observed that the object generated by the SLM does not produce the diffraction pattern with desirable quality, mainly due to the lack of contrast in the image generated by the SLM.

7.2 Further Study

The results of the simulations are qualitatively discussed for the optical display of transient wave propagation. These simulations do not provide the calibration factor that enables us to relate analogous variables; specially, the time variable and the sampling location of the intensity. Further study is needed so that a quantitative analysis of the optical display method can be made as well.

7.3 System Improvement

One of the main sources of error in the experiments discussed in this thesis can be identified as the inaccurate data reading caused by the lack of high output intensity. As explained in the previous chapters, a pin-hole is located in front of the photo-detector for effective sampling of intensity variation; however, it decreases the amount of intensity captured by the photo-detector. In order to maintain the degree of accuracy for the output reading without lowering the intensity by the pin-hole, a high resolution one-dimensional photo-detector array can be used instead of a photo-detector. Combined with an appropriate spatial filtering and the numerical analysis of post-sampling process, the array of photo-detector cells can perform the parallel reading of the output intensity without having to distinguish the sampling location one-by-one. It can also reduce the error occurring when translating the detector.

REFERENCES

1. A. W. Lohmann, J.Ojeda-Castaneda and J. G. Ibarra, " Airy function and Laguerre polynomials: Optical display and processing ," *Optics Communications*, Vol 109, pp 361-367, 1994.

2. A. W. Lohmann and J.Ojeda-Castaneda, " Bessel function: parallel display and processing," *Optics Letter*, Vol 19, pp 55 - 57, 1994.

3. A. W. Lohmann, J.Ojeda-Castaneda and A. Serrano-Herdia, " Trading dimensionality in signal processing," *Optics and Laser Technology,* Vol 28, pp 212-217, 1996.

4. A. W. Lohmann, J.Ojeda-Castaneda and A. Serrano-Herdia, "Synthesis of 1D complex amplitudes using Young's experiment," *Optics Communications*, Vol 101, pp 17- 20, 1993.

5. A. W. Lohmann and J.Ojeda-Castaneda, " Computer generated holography: novel procedure ," *Optics Communications,* Vol 103, pp 182 - 184, 1993.

6. T.-C. Poon and P. P. Banerjee, Principle of Applied Optics. Aksen Associates Inc. Bostin MA, 1991.

7. J. W. Goodman, Introduction to Fourier Optics. McGraw-Hill, New York, 1968.

8. M. Abramowitz and I.A. Stegun, Handbook of Methematical Functions. Dover, New York, 1970.

9. J. D. Gaskill, Linear Systems, Fourier Transforms, and Optics, John Wiley and Sons, New York, 1978.

10. R. G. Willson, Fourier Series and Optical Transform Techniques in Contemporary Optics, Wiley - Interscience, New York, 1995.

11. K. Sigmon, MATLAB Primer, University of Florida, Gainesvliie, FL, 1993.

12. C. M. Thompson and L. Shure, Image Tool Box User's Guide , Math Work Inc. Natick, MA., 1993.

13. S. Wolfram, Mathematica - a system for doing mathematics by Computer, Addison-Wiley, New York, 1991.

14. J. L. Horner, Optical Signal Processing, Academic Press Inc., San Diego, 1987.

15. L. J. Cutrona, ed J. T. Tippet, " Recent Developments in Coherent Optical Technology", in Optical and Electro Optical Information Processing, MIT press, Cambridge, 1965.

16. Francis T.S. Yu and I.C. Khoo, Principles of Optical Engineering, John Wiley and Sons, New York, 1990

17. M.E. Sockell, "Phase-Space Analysis of Wave Propagation in Homogeneous Dispersive Media and its Relationship to Catastrophe Theory", M.S. thesis, Virginia Polytechnic Institute and State University, Blacksburg, VA, 1983

18. G.B. Whitham, Linear and Nonlinear Waves, John Wiley and Sons, Inc. New York, 1974.

19. Product Information sheet provided for the EBSLM model X3636, provided by Hamamatsu Photonics K. K., Japan through Hamamatsu Corp., Bridgewater, NJ., 1989

20. B. W. Schilling, "Advances in Real-Time Optical Holography ," M. S. thesis, Virginia Polytechnic Institute and State University, Blacksburg, VA, 1992.

21. Electron Beam addressed Spatial Light Modulator (EBSLM), Model X3636, provided by Hamamatsu Photonics K. K., Japan through Hamamatsu Corp., Bridgewater, NJ, 1989.

22. R. A. Gayakwad, OP-AMPs and Integrated Circuits, Prentice-Hall International Inc. Eaglewood Cliffs, 1988.

23. EBSLM Controller, Model C3637, provided by Hamamatsu Photonics K. K., Japan through Hamamatsu Corp., Bridgewater, NJ, 1991.

APPENDIX A

```
function cube2(x)

%-------------------------------------------------------------------
% Creates the image of y=(alpha)*x.^3 and FFT the image by cube2(x).
% X : INPUTs, the sampling number on x-axis
% i.e.) x=50 : 2*50=100 sampling points applied.
%-------------------------------------------------------------------

hs=512;  % SIZE of the image matrix.

h=zeros(hs,hs);    % declaration of the image matrix 'h'

y=1/3*x.^3;          % MAX. value of Y_axis.

xi=1:1:x;        %RANGE of X_axis.
yi=1/3*xi.^3;        %Y_axis' range.

step_x=2*x./hs;   % SiZE of each STEP increasing on X, and Y axis.
step_y=2*y./hs;

x_new=xi./step_x;  % creating a new array corresponding to the matrix size 'hs'.
y_new=yi./step_y;

for i=1:1:x;
  h(hs/2+1-y_new(i),x_new(i)+hs/2)=1;
  h(y_new(i)+hs/2,hs/2+1-x_new(i))=1;
end

colormap(gray(64))
% imagesc (h)       % plotting the object pattern ((T(x,y))
%^^^^^^^^^^^^^^^^^^^^^^^^^^^^^^^^^^^^^^^^^^^^^^^^^^^^^^^^^^^^^^^^^^^^^^^^^^^^^^

g=gaus2;             % intro. of 1D GAUSSIAN function.

hm=h.*g;
fcon=fftshift(fft2(fftshift(hm)));  % FFT2 of the object

%==================================================================

% Using the cubic spline interpolation, the COIP (Cut-Off Intensity Pattern)
```

```
% of the processed image can be plotted.

 y_p1=128;     ;              % the POSITION of DIRAC DELTA function on x-axis
 y_p2=115;
 y_p3=100;


x1=110; x2=140;                % RANGE of x vector of interpolation function.
 x=x1:x2;                % setting up the sampling position of DIRAC DELTA function.

sx=size(x,2);

fcon=fcon.*conj(fcon);          % calculates the intensity

norm=31500;             % normalization factor


y1=fcon(y_p1,x)/norm;      % y vector for cubic-spline interpolation
y2=fcon(y_p2,x)/norm;
y3=fcon(y_p3,x)/norm;



xi=x1:0.1:x2;              % x vector for cubic spline interpolation
 %
yi1=spline(x,y1,xi);       % Applying Cubic Spline Interpolation.
yi2=spline(x,y2,xi);
yi3=spline(x,y3,xi);

plot(xi,yi1,'c:',xi,yi2,xi,yi3,'y--')%,grid       %PLOT COIP of the FT(image).

text(130,0.9,'Time=t0')
text( 121,0.6,'Time=t1>t0')
text(120,0.3,'Time=t2>t1')
text(112,0.9,'.... t=t0')
text(112,0.8,'__ t=t1>t0')
text(112,0.7,'- - t=t2>t1')
%xlabel('time');
ylabel('Normalized Intensity Magnitude');
```

```
function g=gaus2

%-------------------------------------------------------------------
%  creates 1-D Gaussian function with a desired parameters
%  output : a 1D gaussian matrix
%-------------------------------------------------------------------

k=0.5;                  %gaussian parameter
%p=512*2/1.23;          %adjustment factor
%k=k/p;

a=sqrt(2*pi);  % constant
c=512;         %size of the matrix
d=c/2;

g=zeros(c,c); b=d;

 for i=1:.1:b;


        x=abs(b-i); %y=abs(b-j);


        g(d,d-x)=a*exp(-k*(x.^2));

        g(d,d+x)=a*exp(-k*(x.^2));


 end

r=rect2;                        % calling a rectangular function
g=conv2(g,r,'same');   %convolution with a rectangular function
```

```
function r=rect2

% creates a 1D rectangular function

m=512;          % size of the rectangular function
s=512;                  % size of the image matrix

r=zeros(s);

for i=1:1:m;
        r(i-m/2+s/2,s/2)=1;

end

%colormap(gray(64));

%imagesc(r)
```

VITA

Mr. Jeong-Han Kim was born in Seoul, South Korea, on January 1, 1969. From the Fall of 1987 to the Spring of 1989, he went to Yonsei University in Seoul and studied Civil Engineering. In the Spring of 1993 he received his Bachelor's degree from Southern Illinois University at Carbondale, Illinois, in Electrical Engineering. He is currently pursuing a Master's of Science degree in Electrical Engineering at Virginia Polytechnic Institute and State University.